Developing drug screening methods using a zebrafish model of motor neurone disease

Madelaine Tym

A thesis submitted in partial fulfilment
of the requirements for the degree of
Master of Research

MACQUARIE
University

Faculty of Medicine and Health Sciences
Macquarie University
Date: 11/12/2019

Word Count: 15829

DECLARATION

Except where appropriately acknowledged, the material presented with this thesis is the result of the candidate's own research and it has not, nor any part of it, been submitted for a degree to any other university or institution.

The research resulting from this thesis was performed in the absence of any commercial of financial conflicts of interest.

The research conducted for this for this thesis was performed with approval from the Macquarie University Animal Ethics Committee (see appendix A). All experiments were conducted using protocols approved by the Macquarie University Animal Ethics Committee.

Signature:

Candidate: Madelaine Tym

Date: 11/12/2019

ACKNOWLEDGEMENTS

I'd like to start out by thanking anyone that helped me, even slightly, all this year.

It was a crazy year for me:

My dog broke her leg the weekend before I was due to start,

I had one of my closest friends leave work,

At one point I also had some valuables stolen out of my car,

I moved to a new house during the middle of my candidature,

And, I was also unlucky enough to lose two of my grandparents.

At least I didn't also have a thesis to finish…

Which is why I'd like to start off by thanking my incredibly supportive family, particularly my parents for helping me move into theirs and providing unending care and support while I finished my thesis. Thanks especially to mum for helping and supporting me through the actual writing process.

I'd also like to thank everyone in the fish room who help take care of the fish: Jason, Cheryl, Bridget, German, Hayley and Tuugsuu. All your hard work through the year is endlessly appreciated.

I'd like to thank everyone in the lab: Maxinne, Luan, Kristy, Isabella, Zac, Natalie, Marco, Adam and Andres. All your help and support was amazing. I'd like to thank Caitlin, thanks so much for all the little things you helped me with this year, I missed you in the lab after you left, but am glad you are enjoying your new job! Thanks also Katie, words literally can't explain how helpful you were this year. Real MVP.

I also can't thank my supervisors enough. Emily thanks so much for your support this year it really meant a lot. Angela thanks so much for all your help and guidance this year it was truly appreciated.

I also just need to take the time to say some things for myself, this year was very difficult for me, because as my grandfather was passing, the family found out it was a strong possibility it was MND, although they couldn't say for sure. Either way it was very confronting watching

him pass, in a manner that I know was the same as how those with MND pass. I'm eternally grateful to the ICU staff at the Northern Beaches Hospital, who were able to keep him stable until my aunt and father arrived back from overseas, in order to say goodbye properly. It's also one of the reasons I found it so difficult to continue working in the lab on a method (primary cell culture) I was struggling to get right.

I'd also like to thank anyone that had any contribution to the idea of me trying flow cytometry directly, including Katie, Maxinne, Angela, and myself as well!

I refuse to end my acknowledgements on such a sad note however, because I can't but help try to inject humour into any situation. To those about to read this thesis, I hope you like the words methods, investigation, and aggregation…. Enjoy.

This thesis is dedicated to my papa Jim Harrison, and my grandfather Tony Tym. I know you'd both be proud.

ABSTRACT

The FUS protein is a nuclear DNA/RNA binding protein that regulates gene expression and that when mutations occur in this protein it can aggregate and contribute to MND pathology. This project aimed to test the effect of treating transgenic zebrafish larvae expressing mutant FUS-R521C-GFP protein with drugs that induce the autophagy pathway. Different methodologies were used to examine whether these drugs can aid removal of FUS aggregates and decrease levels of mutant FUS protein. Treatments with spermidine saw a decrease in FUS-R521C-GFP protein with western blot analysis and a decrease in aggregation with flow cytometry analysis.

Table of contents

List of Figures

List of Tables

1. Introduction

1.1. Investigating FUS aggregation in MND

Amyotrophic Lateral Sclerosis (ALS) also known as motor neurone disease (MND) is a fatal neurodegenerative disease caused by the death of motor neurons in the central nervous system (CNS) (van Es et al., 2017). This results in an inability to control muscle movement leading to eventual death, typically when patients lose the ability to control respiratory muscles (Bonafede & Mariotti, 2017). The pathogenesis of MND is poorly understood. Some cases of MND (around 10%) are known as familial ALS (fALS) and are genetically linked and passed down through families (Spires-Jones, Attems, & Thal, 2017). The cause of the remaining 90% of MND cases, known as sporadic ALS (sALS), remains unknown, but are suspected to involve complex genetic and environmental factors (Chiò et al., 2018). One protein known to be mutated in some cases of fALS is Fused in Sarcoma (FUS) (Sharma et al., 2016). FUS mutations are now known to occur in 5-10% of familial MND cases (Kwiatkowski et al., 2009). The most common MND-causing mutations found within FUS occur at the 521st amino acid of the protein (Kwiatkowski et al., 2009; Shang & Huang, 2016). For example, one common patient mutation is FUSR521C, where the arginine located at the 521st position in the protein is mutated, in this case, to a cysteine amino acid (Kwiatkowski et al., 2009).

FUS-positive protein-inclusions are often found in brain pathology samples from MND patients carrying FUS-mutations, and have also been shown to be present in post-mortem tissue in other forms of fALS, as well as sALS (Deng et al., 2010).

The FUS protein is a predominately nuclear DNA/RNA binding protein that regulates gene expression (H. Wang & Hegde, 2019). Regular function of the FUS protein includes localisation to sites of RNA/DNA damage, and in times of stress, FUS localises to the cytoplasm (Patel et al., 2015). The FUS protein has a low-complexity binding domain, which enables it to act as a liquid, and form a ‘liquid compartment’ to bind to DNA/RNA (Murakami et al., 2015; Patel et al., 2015). It is thought that the structure of the FUS protein could account for its propensity to aggregate when mutated, and it has been shown that higher concentrations and certain mutations can lead the protein to form aggregates and stress granules, rather than remaining in a liquid state (Acosta et al., 2014; Bosco et al., 2010; Patel et al., 2015; Schwartz, Wang, Podell, & Cech, 2013). This build-up of insoluble protein aggregates in cells is a

hypothesised cause of the death of motor neurons in MND making FUS an important target in studying this disease. (reviewed in Spires-Jones et al., 2017).

1.2 Models of MND using mutant FUS

1.2.1 Mus Musculus and *Rattus Norvegicus*

A common animal model used to study neurodegenerative disease are rodents, namely *Mus musculus* (mice) and *Rattus norvegicus* (rats), these animal models are advantageous as they are mammals and are therefore more similar to humans than small animal models such as zebrafish, flies or nematodes (Guigó et al., 2003; Janus & Welzl, 2010). One previously reported rat model that overexpressed mutant human FUS demonstrated that expression of mutant FUS resulted in FUS aggregation and mislocalisation of FUS to the cytoplasm, along with fragmentation of the golgi apparatus and mitochondrial aggregation (Huang et al., 2012). This rat model more closely modelled another linked disease, frontotemporal lobar degeneration (FTLD) rather than MND, as the rats experienced memory loss, and motor neuron degeneration was not reported. However, this model still reveals important information on the role that mutant FUS plays in a mammal animal model. Golgi fragmentation has also been observed in MND patients and this phenotype has also been reported in SOD1 mouse models of MND/FTLD (Fujita & Okamoto, 2005). Two additional papers that experimented with mouse models of over-expressing mutant human FUS have found that FUS mislocalised to the cytoplasm and caused toxic gain of function effects (Scekic-Zahirovic et al., 2016; Sharma et al., 2016). These papers both used FUS knockout mice compared to the mouse model with cytoplasmic mislocalised mutant FUS. Neither paper observed motor neuron loss in the FUS knockout mouse model, which experienced depleted levels of FUS in the nucleus. In comparison both papers found their cytoplasmic mislocalised mutant FUS mouse model experienced motor neuron degeneration and death (Scekic-Zahirovic et al., 2016; Sharma et al., 2016).

1.2.2 Drosophila Melanogaster

Drosophila are a useful animal model for studying neurodegeneration. The shorter lifespan of flies allows important questions regarding disease pathogenesis to be answered more quickly than in rodent models (McGurk, Berson, & Bonini, 2015). The toxic gain of function mechanism of mutant FUS proposed in rodent models has also been demonstrated in drosophila

models (Lanson Jr et al., 2011). This was expanded upon in a drosophila model which expressed the human mutant FUS protein with a mutated nuclear export sequence (NES) that suppressed the toxicity associated with mutant FUS (Lanson Jr et al., 2011). This set of experiments provided more evidence that mislocalisation of FUS due to MND-linked mutations causes a gain-of-toxic-function effect (Lanson Jr et al., 2011).

1.2.3 Caenorhabditis Elegans

Another important scientific animal model is the nematode invertebrate *Caenorhabditis elegans* (*C. elegans*). *C. elegans* have a short life cycle of about 10 days and are transparent, making them useful models of neurodegenerative disease (Wolozin, Gabel, Ferree, Guillily, & Ebata, 2011). *C. elegans* have been used to model a variety of different proteins known to cause MND, such as TDP-43, SOD,1 as well as FUS (Li, Huang, & Le, 2013; Murakami et al., 2012; Vaccaro, Patten, et al., 2012; Vaccaro, Tauffenberger, et al., 2012).

Experiments conducted using *C.elegans* have shed further light on the role of FUS in MND pathogenesis (Murakami et al., 2012). One paper found that over expression of mutant FUS, also caused mislocalisation of FUS to the cytoplasm in a similar fashion to that observed in rodent models (Murakami et al., 2012; Nolan, Talbot, & Ansorge, 2016). Further, this model also exhibited motor dysfunction and had a shorter lifespan (Murakami et al., 2012). Additional studies using this model showed that mutations in FUS that cause rapid disease progression in MND patients also produce more severe phenotypes in the *C. elegans* model. This has provided an argument that this model is a good replicate of the disease as it is found in humans (Murakami et al., 2012). This study also found that the phenotype could not be rescued through expressing FUS-WT, which does localise to the nucleus, and was not found in the cytoplasm at all (Murakami et al., 2012). This study also suggested a dominant gain-of toxic function effect, potentially related to dysfunction in its RNA-binding functions or the neurotoxic aggregates formed (Murakami et al., 2012) This argument is supported by an additional study which expressed mutant FUS within the *C. elegans* GABAergic motor neurons and showed similar results of insoluble protein misfolding, cytoplasmic mislocalisation, an adult-onset loss of motor function and progressive paralysis and neuronal degeneration. (Vaccaro, Tauffenberger, et al., 2012).

Whilst *C.elgans* models have provided valuable disease insights and recapitulate findings from rodent models there are some limitations to the *C.elgans* system. These models are non-

vertebrate and their short lifespan possibly makes the study of an a adult onset neurodegenerative disease inappropriate (Wolozin et al., 2011). However, they also validate findings from other models of the toxic-gain-of-function effect mutant human FUS can cause.

1.3 Danio Rerio

Zebrafish (*Danio rerio*) were first used as a research tool as early as the 1950's and gained greater popularity in the 1980's (Bradford et al., 2017). Use of the system skyrocketed during the 1990's due to advances in transgenic technologies, at which point the journal Zebrafish was established (Collodi, 2004). Whilst originally used mostly for studying development, zebrafish are useful research animals, most notably due to their external fertilisation and the rapid development of the transparent embryos (Hammerschmidt & Nusslein-Volhard, 1993; Phillips & Westerfield, 2014). Zebrafish are also, genetically speaking, well suited for use as models of human diseases, including neurodegenerative diseases, as approximately 70% of human genes have a zebrafish orthologue (Gibert & Ward, 2013; Howe et al., 2013; Phillips & Westerfield, 2014; Singer et al., 2016; Xi, Noble, & Ekker, 2011).

To further investigate the effect that FUS aggregation plays in the pathogenesis of MND this project aimed to use an established FUS zebrafish model that utilises stable overexpression of GFP tagged human FUS carrying a common patient mutation (R521C). This model shows dynamic protein aggregates in cells of young embryos which can be visualised with fluorescence microscopy (characterised previously in Acosta et al., 2014). The FUS protein is expressed in a ubiquitous manner, using a beta actin (actb2) promoter. This fish line, Tg(actb2:Hsa.FUS_R521C-EGFP), referred to as FUS-MT throughout the text, was invaluable for this research project. The FUS-MT Zebrafish model displays cytoplasmic mislocalisation of the FUS protein and develops aggregates, making it a useful model of the pathogenesis of MND (Acosta et al., 2014).

This project aimed to characterise and further understand the aggregation phenotype these zebrafish larvae present and investigate whether drug treatments can reduce the amount of protein aggregation in treated vs untreated zebrafish larvae.

1.4 Zebrafish adoption to cell culture

A crucial part of studying MND is being able to analyse the neurons and cellular pathologies of the model to be studied. One method to achieve this with zebrafish larvae is to dissociate

whole zebrafish embryos in order to create a primary cell culture consisting of zebrafish cells (Jamie R Acosta et al., 2018; Sakowski et al., 2012). This is an important method as it allows application of a range of methods suitable for cell culture that are impossible to perform on live animals. It is also possible to enrich these cell cultures for neural cells. These enriched cell cultures derived from zebrafish larvae were first established as a protocol in 2012 (Sakowski et al., 2012). While previous protocols had described culturing of zebrafish embryos to primary cell culture, none had so far described enriching for motor neuron cell types (Andersen, 2001; Sakowski et al., 2012). A key step in this protocol was using only the body and tail of the zebrafish larva and dissecting the anterior portion with fine forceps of the zebrafish larva before dissociation to enhance spinal motor neuron density in the final culture (Sakowski et al., 2012).

Recently the primary cell culture method was modified to skip the initial dissection of the embryo and instead use a slow microsuction technique to remove the yolk from the embryo (Acosta et al., 2018). This study found that the yolk sac removal technique resulted in motor neurons with poor morphology indicated by shorter neurites seen (Jamie R Acosta et al., 2018). In an effort to develop high-throughput methods, based on these results, it was decided not to dissect the larvae before culturing and to keep the yolk sac (Jamie R Acosta et al., 2018; Sakowski et al., 2012).

1.5 Autophagy

This project aimed to characterise, understand and treat a protein aggregation phenotype in an *in-vivo* model. For this reason, cellular processes involved in protein clearance were investigated. One such process is the autophagy protein quality control pathway.

Macroautophagy, more commonly referred to as autophagy, is a process where an autophagosome, formed from a lipid membrane, will capture aggregated proteins before fusing with a lysosome. The lysosome releases agents to break down the captured proteins to its constituent elements i.e. amino acids. Autophagy is an endogenous process used to degrade longer lived misfolded, insoluble, and aggregated proteins (Mathai, Meijer, & Simonsen, 2017; Ramesh & Pandey, 2017). Studies have suggested that autophagy may be impaired in not only MND but also in other forms of neurodegeneration (Nixon, 2013). It has also been found that the presence of mutant human FUS in neural cells is associated with an impairment in autophagy (Soo et al., 2015). Soo et al have demonstrated that formation of autophagosome is inhibited in neural cells expressing mutant FUS with a common patient mutation FUS R521C

(Soo et al., 2015). This makes autophagy an attractive drug target for the treatment of MND, with the hope that inducing autophagy could help clear the protein aggregates that are, if not the underlying cause of the disease, certainly a significant contribution to it (Mathai et al., 2017; Ramesh & Pandey, 2017). There are many different drugs that have been previously reported to be capable of inducing activity of the autophagy pathway. These include rapamycin, spermidine, resveratrol and trehalose (Klionsky et al., 2016). The drug used in this project is spermidine, which is a naturally occurring polyamine that induces autophagy through the inhibition of some histone acetylases (Eisenberg et al., 2009). Spermidine has been previously shown to restore dysregulated autophagy, and alleviate motor symptoms in MND mouse models (Klionsky et al., 2016; Park et al., 2016; Sacitharan, Lwin, Gharios, & Edwards, 2018; I.-F. Wang et al., 2012). It is hoped that treating the *in-vivo* cultures with spermidine will reduce the aggregation phenotype when measured using flow cytometry or automated imaging systems such as an IncuCyte.

Activity of the autophagy pathway can be investigated using western blot methods by investigating known proteins involved in the autophagy system. These proteins include Lamp2a, and LC3B, when investigated together they can reveal whether or not autophagy has been induced by a certain drug compared to untreated controls. The most important of these proteins are LC3B and p62. LC3B is an autophagosome marker, and an increase in this protein indicates more autophagosomes are present in the sample (Klionsky et al., 2016). p62 protein, in an autophagy context, is found to bind to ubiquitinated proteins (aggregates) when the aggregates are then digested through autophagy, p62 is also degraded (Bjørkøy et al., 2009). Thus p62 is a good marker of autophagic flux and a decrease in this protein within increasing drug conccentration indicates that autophagy has been induced. Other autophagic proteins that could be investigated in the future include lamp2a which is a lysosomal marker, and beclin which is a protein involved in the formation of the initial phagophore, both of which can give a more encompassing look at the role of autophagy with a set of drug treatments (Klionsky et al., 2016).

1.6 Aims

1 Further characterise FUS zebrafish lines overexpressing mutant and wild type human FUS protein.

2 Optimise use of transgenic FUS zebrafish larvae for drug testing including culturing of cells from the zebrafish larvae to allow *ex vivo* drug treatments.

3 Test whether potential drug candidates ameliorate disease phenotypes in the mutant FUS zebrafish larvae *in vivo* and *ex vivo*.

The first aim of this project is to further characterise both mutant and wild type overexpressing FUS lines. Microscopy and western blot can determine pathological characteristics and expression levels. Once this is established, drug testing can begin. The second aim of this research project will involve drug testing using autophagy inducers such as spermidine, which again using western blot, can be used to determine whether FUS has decreased or increased. The third aim is to develop and optimise a more high-throughput method to conduct drug studies on the FUS zebrafish larvae, in the hope of rapidly screening potential drug candidates for MND in the future.

2. Methods

2.1. Zebrafish use

Any use of the Zebrafish was conducted in accordance with Macquarie University Animal Ethics Committee approved protocols. (ARA 2015/034).

2.2. Zebrafish lines utilised

The zebrafish lines used in this project are listed in the table below

Table 2.1. List of zebrafish lines used and their description

Line	Description
Tg(actb2:Hsa.FUS_R521C-EGFP)	Ubiquitous expression of mutant human FUS protein
Tg(actb2:Hsa.FUS_WT-EGFP)	Ubiquitous expression of human FUS protein
Tg(mnx1:BFP)	BFP expression in motor neurons
WT Tab (AB/TU)	Non-transgenic

2.3. Zebrafish embryo collection

Male and female zebrafish were setup overnight in a false-bottom pair mating tank with a plastic divider between them. The next morning the divider was removed to allow for spawning. The eggs that had fallen through the false bottom and were collected using a strainer and rinsed to remove particulates such as scales and fecal matter. The eggs were then stored in a plastic Petri dish in egg water (E3) embryo medium (5 mM NaCl, 0.17 mM KCl, 0.33 mM CaCl2, 0.33 mM MgSO in distilled water) No more than a hundred eggs were placed in each Petri dish.

2.4. Microscopy

For confocal microscopy, a single zebrafish larva was placed in an excess of tricaine (4 mg/mL) for 20 minutes, before being placed in a hardened ring of agarose set in a petri dish, and covered with a new solution of warm agarose and held in place until set. The larva was then imaged under a Leica sp5 upright confocal microscope.

Compound microscopy of zebrafish larva were taken by pre-treating larvae with PTU to enhance transparency then exposing a single larva to tricaine (4 mg/mL) before placing on a glass slide and imaging on an inverted compound microscope (Leica, DMI 8).

Primary zebrafish GFP cell culture images were taken on an EVOS® FL Cell Imaging System (ThermoFischer scientific). Primary zebrafish BFP images were taken using an inverted compound microscope (Leica, DMI 8).

2.5. Western blot

A Pierce® BCA assay kit was first used to determine protein concentration of each sample. Western blots samples were then prepared using Laemmli reducing agent and sample buffer with equal amounts of protein and using water to achieve equal volumes for each sample. Samples were heated at 95°C for 3 minutes. Gel electrophoresis was used to separate out the protein by size using 12% Bis-Tris SDS-page gel (NuPAGE, Life Technologies) using MES buffer at 110 volts until protein reached the end of the gel. An overnight wet transfer using Criterion^{TM} Blotter (BioRad) was used to transfer the protein to a nitrocellulose membrane (BioRad), before blocking in 5% skim milk in Tris buffered saline (TBS) buffer (20 mM Tris, 500 mM NaCl, pH 7.5) for an hour. The membrane was incubated overnight in primary antibody. The next day the membrane was washed three times in TBS for 5 minutes before incubation in secondary antibody for 1 hour. The membrane was then washed twice in TBS-Tween (0.005% Tween-20, TBS) and once with TBS for 5 minutes before imaging.

The western blots were imaged on a Licor Odyssey system, which enables dual colour detection using two different wavelengths (680nm and 800nm) depending on which IRDye secondary antibody is chosen. This allowed for the western blot to be probed first using a GFP primary antibody on the 680nm wavelength (using appropriate 680nm secondary antibody) and then allows the western blot membrane to be re-probed for the same protein using a FUS primary antibody, except using the alternate 800nm wavelength secondary antibody for imaging.

For the spermidine drug treatments analysis comprised of normalising the quantified amount of protein to the GAPDH loading control. Quantified values for each replicate were then normalised to the untreated FUS-MT values, before statistical analysis and graphing.

2.6. Drug treatment of zebrafish embryos

After embryo collection, at 1 dpf, thirty zebrafish embryos for each treatment group were dechorionated with Dumont #5 watchmaker forceps (World Instruments). Embryos for each treatment group were then placed into a separate small Petri dish containing a specific concentration of drug dissolved in identical volumes of E3. Appropriate non-transgenic and

non-treated controls were used. The embryos were incubated overnight at 28°C before undergoing protein extraction or flow cytometry at 2 dpf.

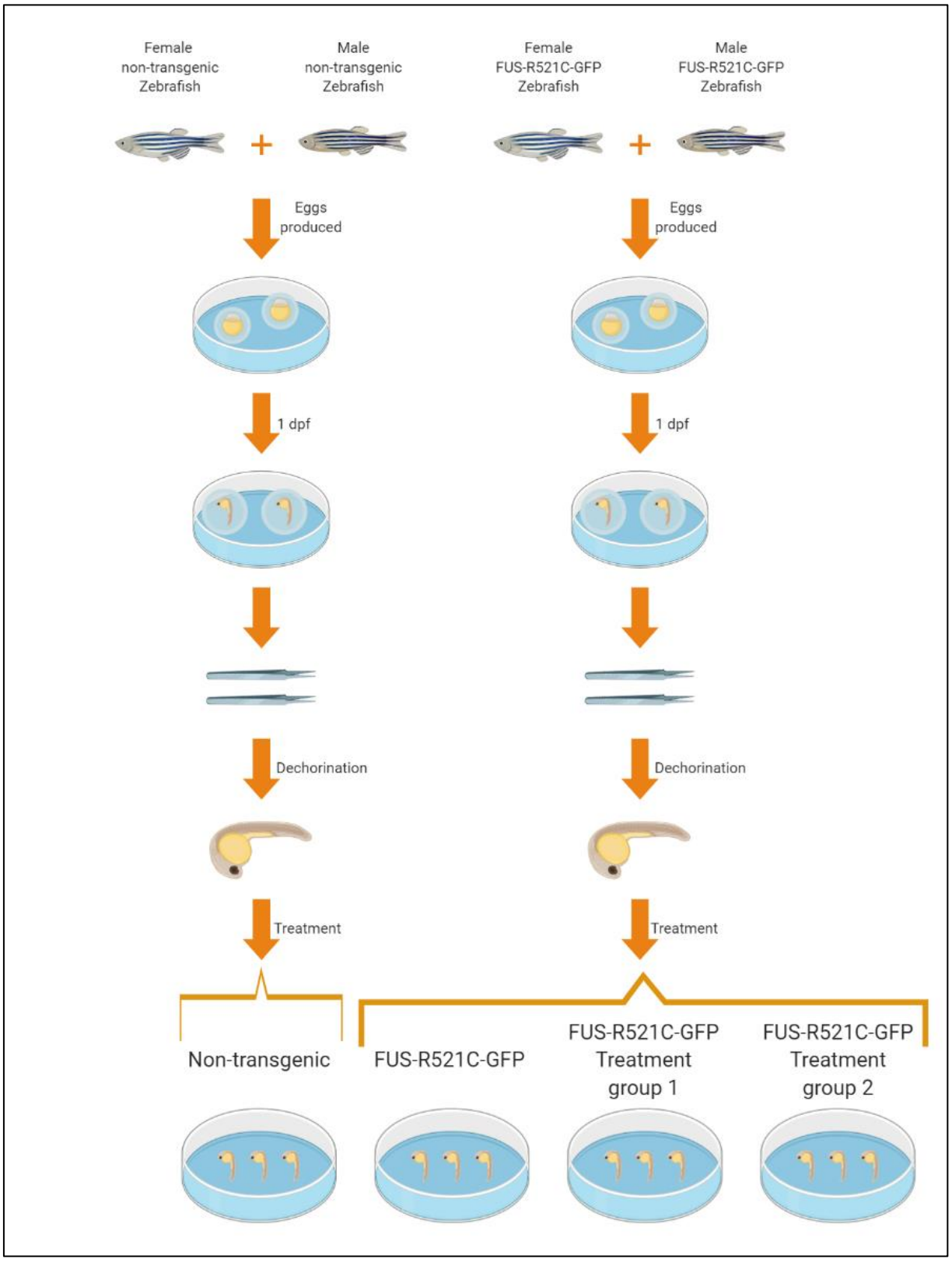

Figure 2.1. Schematic depicting zebrafish embryo drug treatment methodology

2.7. Protein extraction of zebrafish embryo

At 2 dpf the embryos from one treatment were placed into a microcentrifuge tube and washed with E3 before being placed on ice for 15 minutes to be euthanized. All E3 was then removed from the Eppendorf before adding 2µL per embryo of Ringers calcium free medium (116mM, NaCl, 2.9mM KCl, 5 mM HEPES, pH 7.2) and pipetting with a p200 pipette, until the yolk sac's of all embryos were removed. The embryos were then centrifuged at 4°C for 5 minutes at 1,500 x g. The supernatant was then removed. The embryos were then washed by adding 2µL per embryo of phosphate buffered saline (PBS) to the microcentrifuge tube before centrifuging again using the same settings. The PBS supernatant was then removed and 0.5µL per embryo of T-PER^{TM} Tissue Protein Extraction Reagent, (ThermoFischer scientific) or when specified, RIPA buffer, was added to the microcentrifuge tube containing the embryos. Both T-PER and RIPA were prepared with protease inhibitor cocktail (Roche). The embryos were then manually crushed using a dounce, before being centrifuged at 4°C for 20 minutes at 13,000 x g. The supernatant containing the protein was then removed and stored at -80°C to be used in western blots.

2.8. Primary cell culture of zebrafish embryos

At 1 dpf, 25 embryos were selected and washed 3 times with sterile E3 in a TC hood. A solution of E3 containing Penicillin-Streptomycin (Pen-Strep) was then added to the embryos. The embryos were then incubated at 28°C in for 5 hours. The embryos were washed in sterile E3 three times in a TC hood before being washed in 0.005% bleach for 2 minutes. The embryos were then washed in E3, before adding Tricane methanesulfonate (4 mg/ml) to the embryos and placing on ice for 15 minutes to euthanize zebrafish larvae. The embryos were washed in E3 before adding 1x pronase for chorion removal. The embryos were incubated at 37°C for 5 minutes with occasional agitation until chorion removal could be seen. The embryos were then washed 3 times in sterile E3. All E3 was removed and 100µL of 1X trypsin was added with vigorous pipetting to aid dissociation. The embryos were incubated in a 37°C water bath for 15 minutes with intermittent pipetting to aid dissociation of the embryos. Once no embryo remains could be seen 400µL of DMEM with 10% FCS to arrest trypsinization. The mixture was then pipetted slowly to ensure homogenization of trypsin and DMEM. The mixture was then spun at 1000g for 5 minutes to pellet cells. 450µL of the supernatant was removed. The cells were then counted using a cell counter by mixing 20µL of the cell mixture

and 20µL of trypan blue. Cells were plated at 70 000 cells per 96 well. 200µL of Neurobasal media was added to each well. Drug treatments were completed the day after plating by adding specified amount of drug to each well.

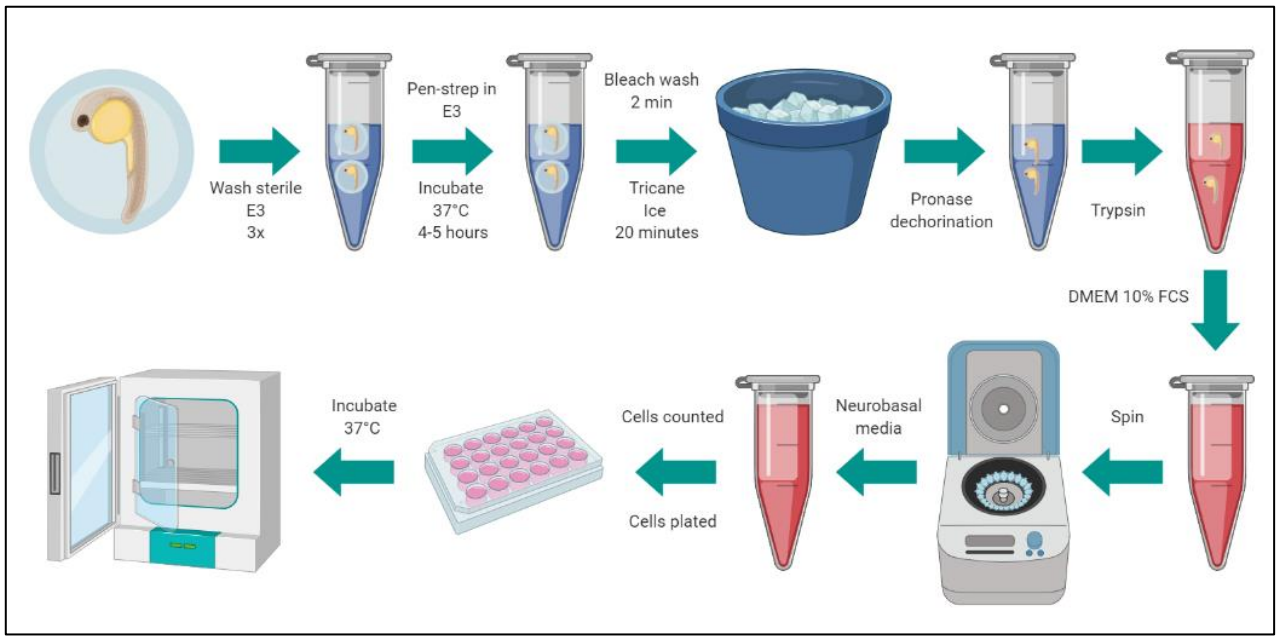

Figure 2.2. Schematic depicting zebrafish embryo cell culture methodology

2.9. Flow cytometry

We then explored developing a protocol to analyse protein aggregate propensity within the mutant FUS zebrafish using a flow cytometry approach performed on zebrafish larva homogenates, without prior cell culture processing. The developed methodology is described in Figure 2.3. At 1 dpf, drug treatments were carried out on the zebrafish embryos. The next day each treatment group of Zebrafish (now 2dpf) were collected and placed in Tricane methanesulfonate for 20 minutes on ice. The Tricaine methanesulfonate was removed and three washes with E3 performed. All embryos were then placed in a small droplet of E3 in a petri dish under a microscope and cut up into smaller pieces or ‘minced’ with a scalpel or tweezers. The minced embryos were collected in a microcentrifuge tube and spun down for 5 minutes at 1,000 x g. The E3 supernatant was removed and trypsin was added to the microcentrifuge tube. The microcentrifuge tube was placed in a heat block at 37°C for 30 minutes, with vigorous pipetting every 3 to 5 minutes. The trypsinization reaction was halted by adding DMEM with 10% FBS. The samples were then spun down at 1,000 x g for 7.5 minutes, and the supernatant removed. The pellet was re-suspended in PBS. At this point a fifth of each sample was removed and diluted 1 in 5, to an appropriate volume for the flow

cytometer, and stained with Hoechst stain (Hoechst 33258, Sigma-Aldrich) to a final concentration of 5 ug/ml, to be run on the flow cytometer. A second aliquot totaling one fifth of the original sample suspended in PBS, again diluted 1 in 5 to be run on the flow cytometer without Hoechst staining. The original samples were spun down at 1,000 x g for 7.5 minutes and re-suspended in PBS with 0.05% Triton X with protease inhibitor cocktail (Roche). This solution was then stained using DAPI before being run on the flow-cytometer.

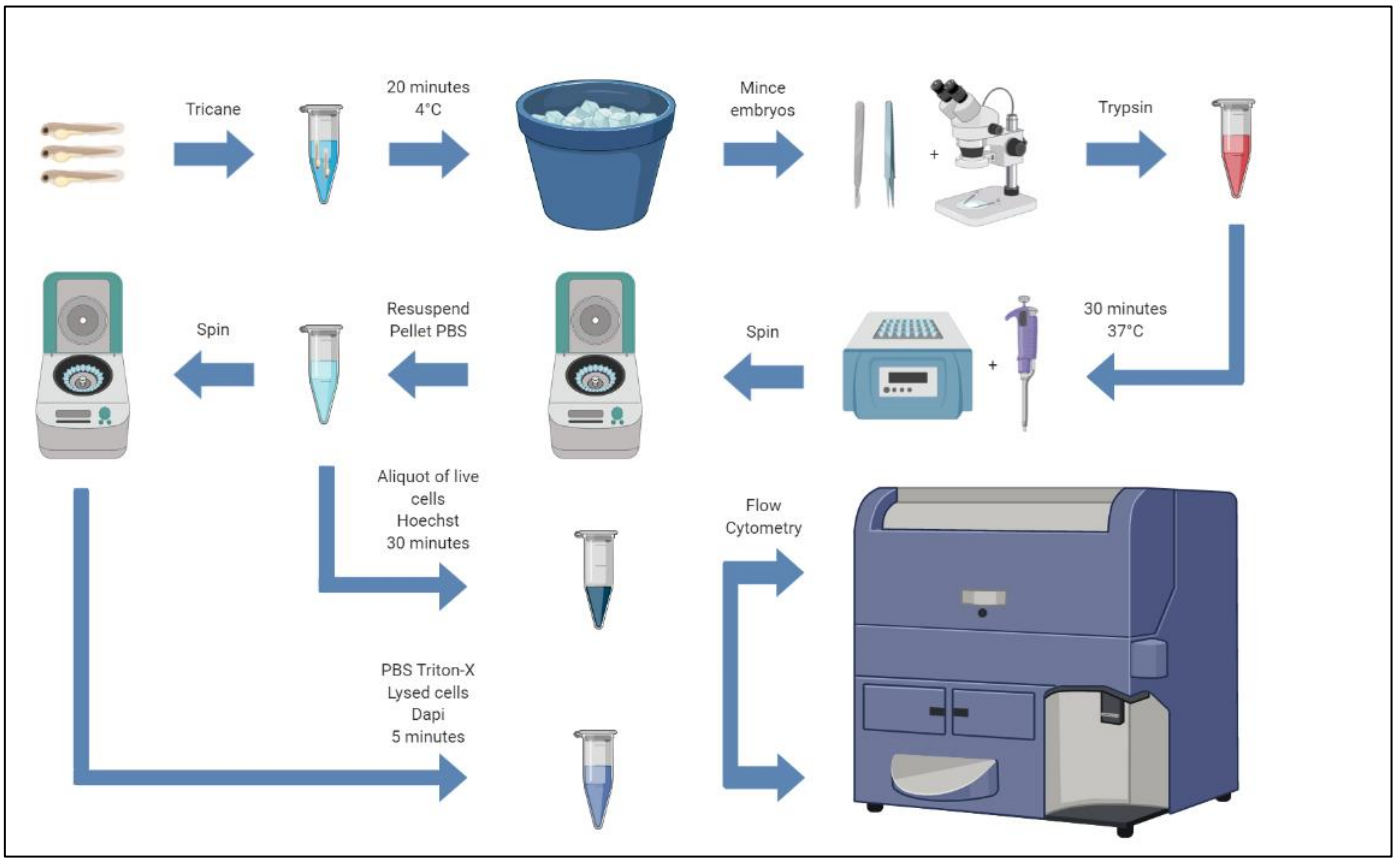

Figure 2.3. Schematic depicting zebrafish embryo flow cytometry methodology

2.10. Flow cytometry analysis for lysed DAPI stained cells

The flow cytometry settings used to capture data for the lysed DAPI-stained samples, had FCS acquisition set to 200, the minimum possible to avoid missing any small particles. For each sample run, 100,000 events were set. Once the lysed DAPI-stained cells were run through the flow cytometer, gating was applied to separate the DAPI-stained particles from the rest of the events captured. In order to do this all particles were graphed according to intensity of UV and FSC. Gating was applied to capture all particles that had high UV expression as seen in Figure 2.4 below. The same gating was applied to each sample.

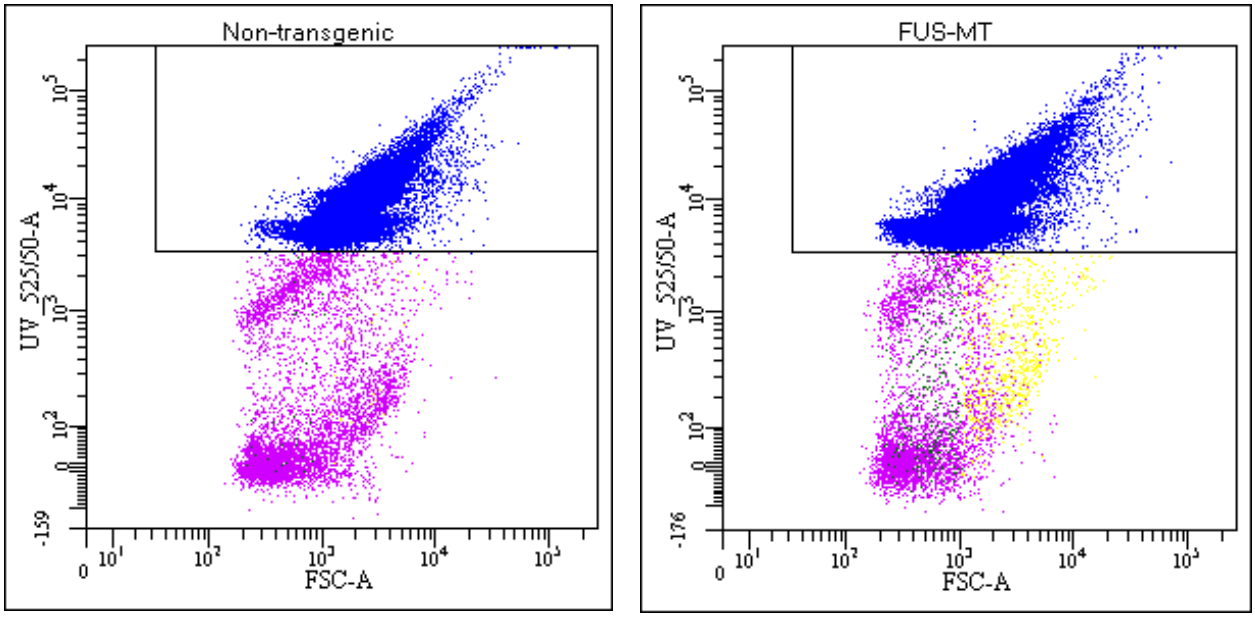

Figure 2.4. Gating example for lysed DAPI-stained samples to capture DAPI-stained particles

In order to then calculate the total number of GFP positive particles, all particles were graphed according to UV and GFP intensity as seen below in Figure 2.5. Particles that were not DAPI-stained were gated (P1 below).

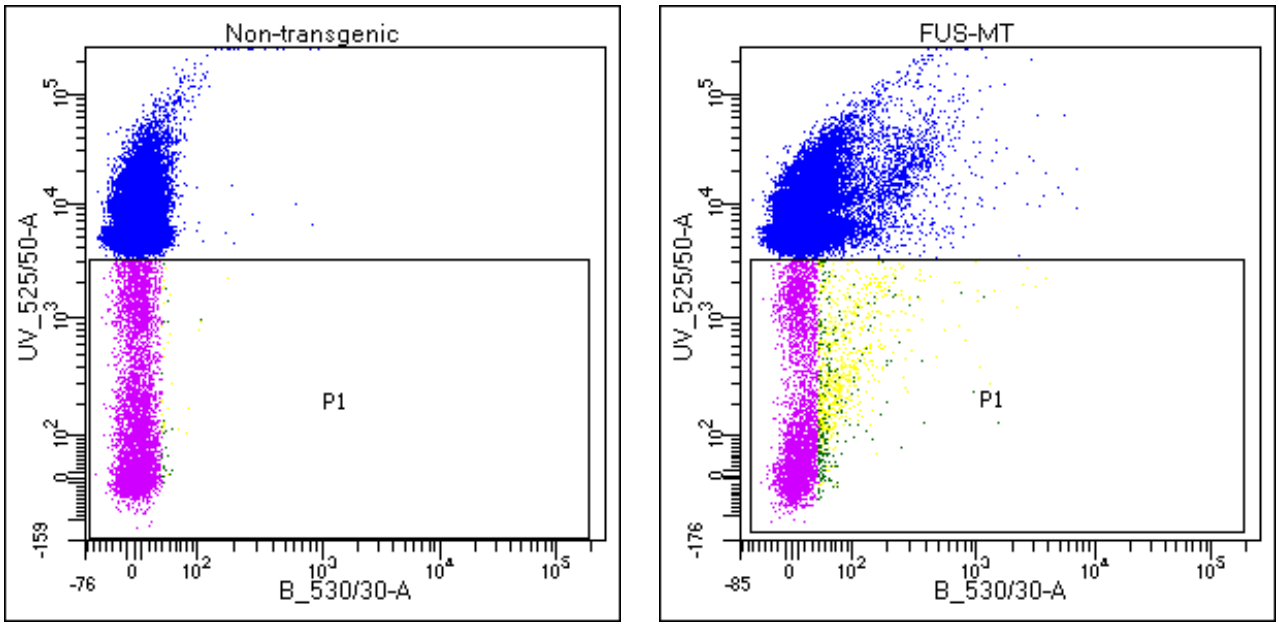

Figure 2.5. Gating example for lysed DAPI-stained samples to capture non DAPI-stained particles

Particles selected from P1 gate were then graphed on a separate plot according to GFP intensity and FSC as shown in Figure 2.6 below. In order to then analyse the size of the GFP positive particles two additional gates were implemented. Gating for this readout required back-gating to the non-transgenic zebrafish larvae sample. Gating was set so that as few as possible of the non-transgenic particles were counted as 'high GFP'. Then two gates were set up, one counting particles larger than 10^3 (P2, designated as 'large particles') and one counting particles smaller than 10^3 (P3, designated as 'small particles').

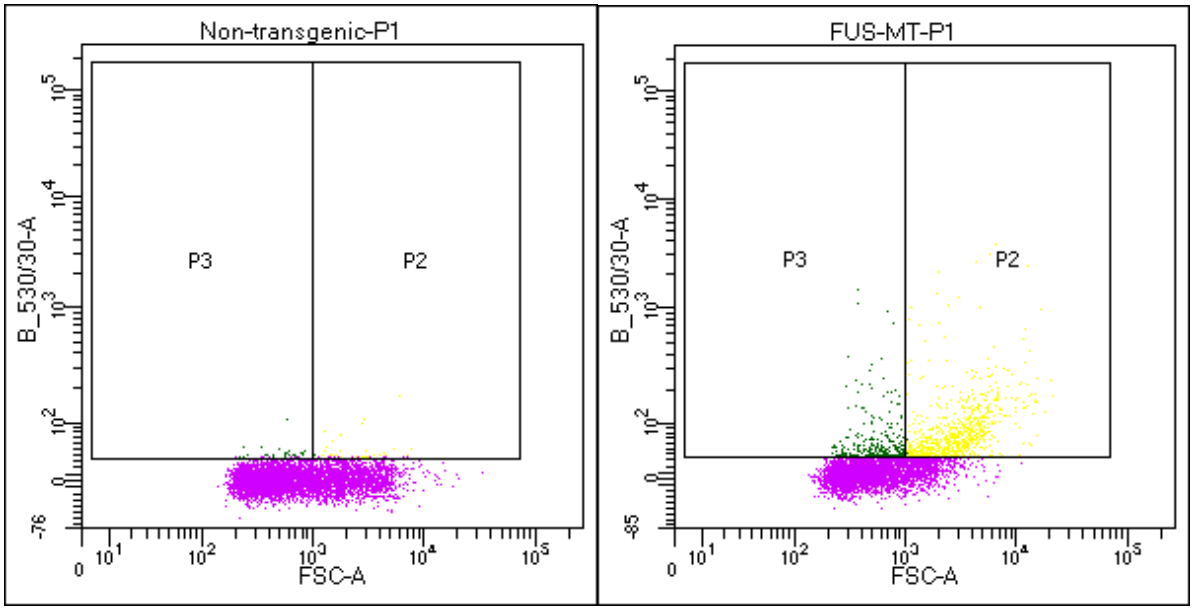

Figure 2.6. Gating example for lysed DAPI-stained samples to capture large and small GFP positive particles

The total number of GFP positive particles was calculated through the addition of particles identified within the small particle gate and large particle gate (P2+P3). The number of GFP particles was normalised to the number of DAPI-stained particles within each sample, followed by graphing of results.

2.11. FloIT analysis and transfection efficiency of Hoechst stained cells

To calculate a value for 'transfection efficiency' for inclusion within the FloIT formula (described above) we calculated the number of green cells present (prior to Triton X-100 lyses to obtain insoluble aggregates) and expressed that number as a proportion of the number of Hoechst positive cells (total cell count). Transfection efficiency here is a relic term from adopting these calculations from the original development of the flow cytometry technique

FloIT which was previously performed in cell culture studies and allowed reporting of the number of inclusions per 100 GFP positive cells (Whiten et al., 2016).

Two approaches were trialled for calculation of this 'transfection efficiency' (or percentage GFP positive cells), one by analysing microscopy images and one using flow cytometry prior to Triton-X treatment.

The flow cytometry settings used to capture data for the whole cell (un-lysed) Hoechst-stained samples, had FCS acquisition set to 5000, in order to count cells. Hoechst staining was used to determine the transfection efficiency of each treatment group. Transfection efficiency was calculated by dividing the number of GFP positive cells by the number of UV positive cells within the 10,000 events counted by the flow cytometer. To ascertain cell count of each fluorescent signal, UV and GFP were graphed against each other as seen below in Figure 2.7. Gating was set based on the fluorescence of the non-transgenic siblings. Transfection efficiency calculations followed the following formula (Q1+Q2)/(Q2/Q4) and expressed as a percentage before graphing.

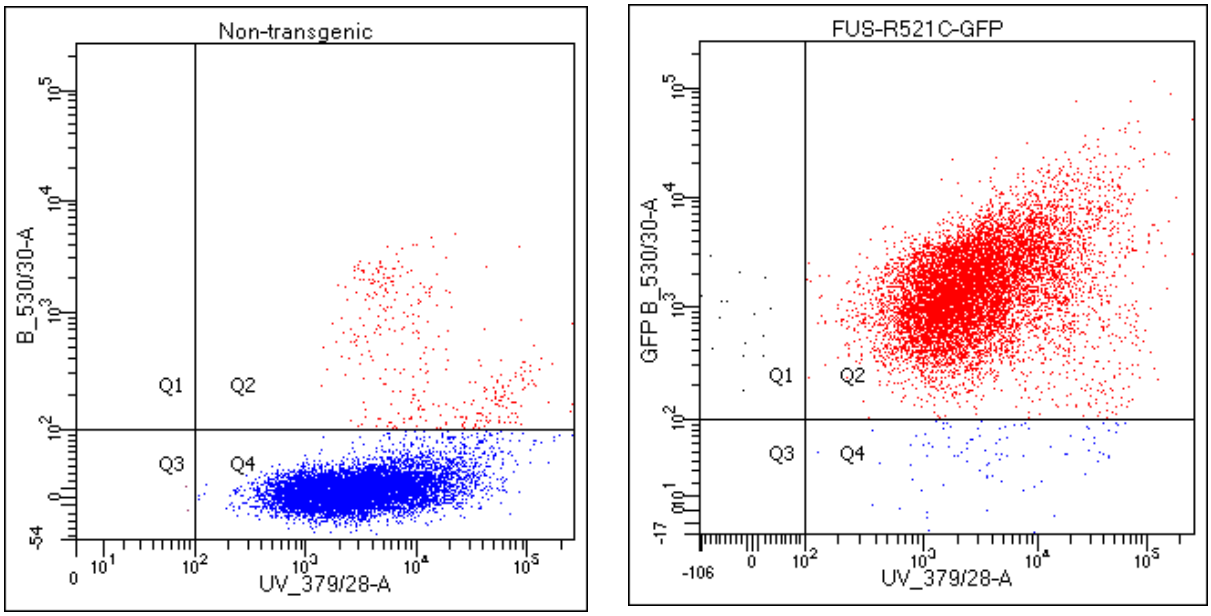

Figure 2.7. Gating example for Hoechst-stained cells to determine transfection efficiency

For microscopy transfection efficiency analysis, an aliquot of Hoechst stained cells was placed under a microscope and imaged on GFP and UV setting on an inverted compound microscope (Leica, DMI 8). The number of GFP positive cells and UV positive cells were counted and expressed as a percentage.

The FloIT process was only carried out with the positive FUS embryos because it produced skewed data for very low positive embryo cohorts. Once the trasnfection efficiency was calculated, FloIT analysis was then applied to the aggregation particle count results, in order to quantify the number of aggregates per 100 positive cells in each sample. The calculation used is as follows:

$$i = 100\left(\frac{n_i}{\gamma \cdot n_{nuc}}\right)$$

where n_i is the number of inclusions present, n_{nuc} is the number of nuclei present, and γ is the transfection efficiency.

2.12. Statistical Analysis

Statistical analysis was conducted using GraphPad PRISM 8.0 (GraphPad software). All statistical analysis for this project originates from at least three independent experimental replicates. All graphs depict mean ± standard error of the mean. All statistical testing was performed using a one-way ANOVA statistical test, followed by Dunnetts post hoc analysis. A statistically significant difference was determined using a value of $p < 0.05$ and statistical significance was denoted using the values $p < 0.05$ (*), $p < 0.01$ (**), $p < 0.001$ (***).

3. Results

3.1. Characterising aggregation and zebrafish fluorescence expression levels between wildtype and mutant overexpression lines

The overall aim of this segment of results was to investigate the cellular and behavioural traits of the mutant human FUS transgenic zebrafish line, this included tracking behaviour and confirming aggregation and line utility.

3.1.1. Using fluorescence to confirm GFP expression level in zebrafish lines

This project utilised two transgenic zebrafish lines which expressed GFP tagged to either a mutant human FUS protein (FUS-MT) or wildtype human FUS protein (FUS-WT). This protein was expressed in a ubiquitous manner throughout the fish, using a beta-actin promoter. The GFP tag in both these lines gives an approximation of expression of the tagged protein, with a higher fluorescence expression level generally indicating a higher level of the tagged protein (Figure 3.1).

This experiment involved taking fluorescence images of zebrafish larvae at 2 dpf from an incross of both FUS-WT and FUS-MT lines as well as an outcross of FUS-MT to a non-transgenic zebrafish, in order to compare GFP expression level.

As seen in Figure 3.1(A) the FUS-WT zebrafish larvae expression level was dim with minimal residual GFP expression only seen in the heart. Compared with this, the GFP expression in the FUS-MT zebrafish larvae, despite the same exposure time, exhibited far greater expression levels than the FUS-WT larvae. Evidently, it is possible that major silencing had occurred over successive generations to the FUS-WT zebrafish, as expression had diminished significantly, since it was previously reported (Acosta et al., 2014).

Figure 3.1(B) also shows that the FUS-MT zebrafish line when outcrossed to a non-transgenic line produced both negative and positive siblings, (useful for providing control animals for studies) as indicated by their relative fluorescence levels. Although these zebrafish larvae were imaged at 2 dpf, the difference in expression levels can be ascertained at an earlier time point 1 dpf in order to begin experiments before this time.

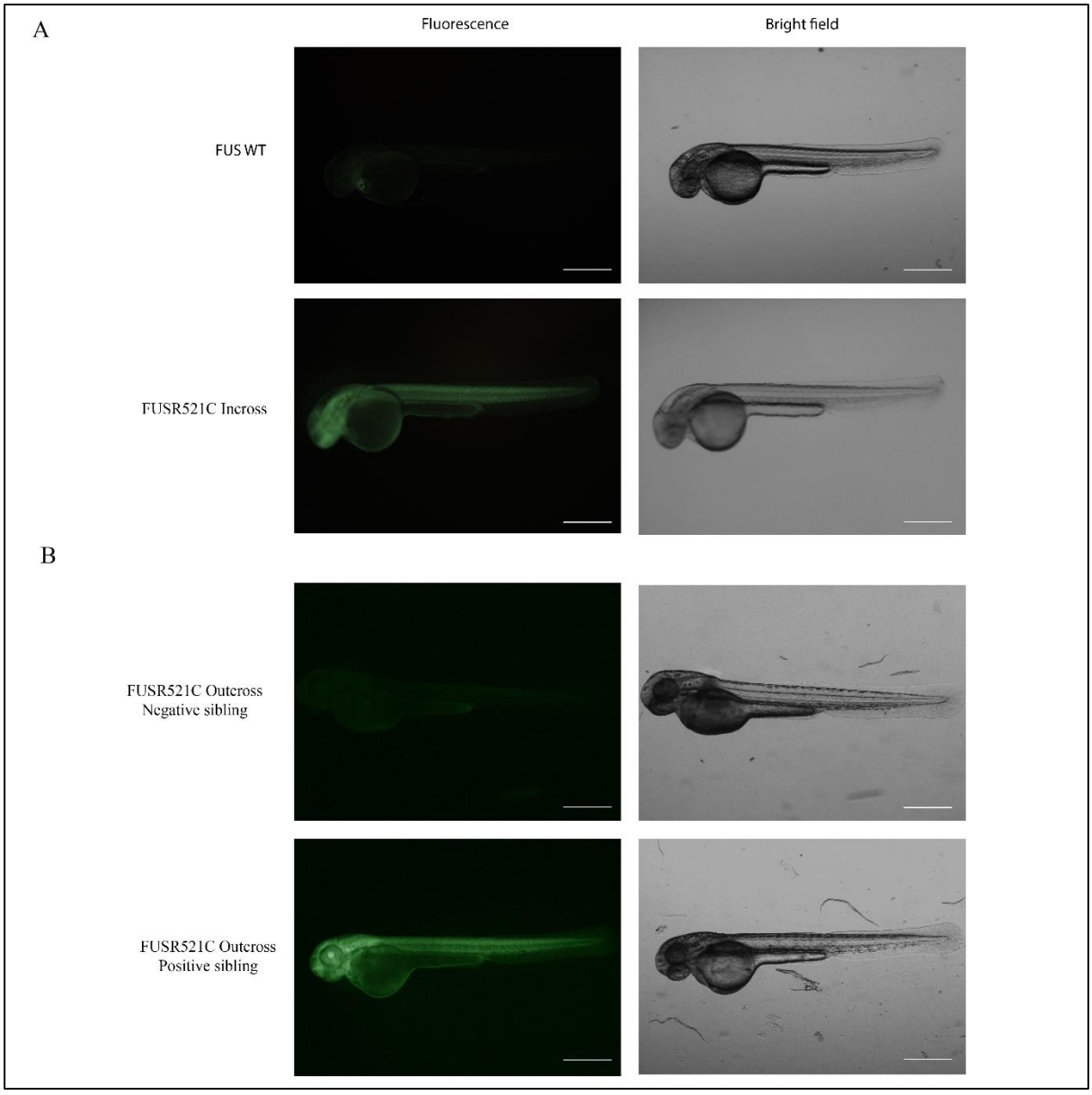

Figure 3.1. The GFP expression levels of FUS-MT and FUS-WT transgenic zebrafish lines

The expression levels of FUS tagged GFP proteins in (A) FUS-R521C-MT fluorescence expression and (B) siblings from a FUS-R521C-MT outcross to a non-transgenic line. Fish were imaged at 2 dpf. Pictures were taken on Leica screening microscope. Exposure for fluorescence and brightfield were consistent between both images in (A) and (B). Scale bar is 500 µm.

3.1.2. Using western blot to confirm FUS expression level in zebrafish lines

The FUS expression analysis was then extended using western blot analysis, where lysates from each zebrafish line were run in parallel to compare protein abundance. This is shown in Figure 3.2 below. The human FUS protein that is expressed in these zebrafish is 75kDa when endogenous, however as the protein is tagged to GFP (25kDa) the expected protein size was 100kDa. Similar band sizes were expected for both the FUS-MT lysates and FUS-WT. It was

also expected that there would be endogenous zebrafish FUS protein lower down on the western blot, as zebrafish have a FUS protein that is smaller, approximately 40kDa (Lebedeva, de Jesus Domingues, Butter, & Ketting, 2017). One advantage of having a GFP tag in the expression construct was the ability to probe separately for GFP protein and the FUS protein to validate findings.

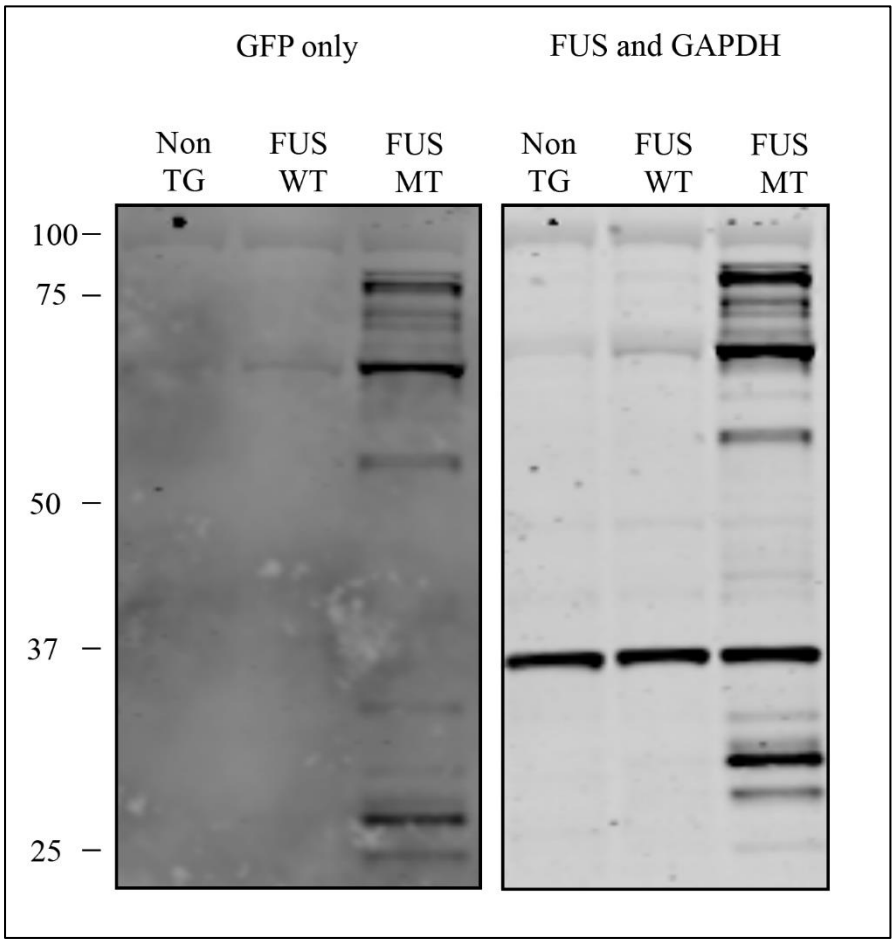

Figure 3.2. Lysates made 2 dpf were optimal for western blots and FUS-MT lysates showed FUS protein despite equal loading.

Western blot of non-transgenic, FUS-WT and FUS-MT lysates showing levels of GFP, FUS and GAPDH as a loading. The GFP only blot shows only the 680nm channel used to image on the licor machine, while the FUS and GAPDH show the 800nm channel image.

The GFP probe in the non-transgenic lysate showed faint bands at 100kDa, and ~65 kDa, while the FUS probe showed faint bands at 100kDa, 75kDa and ~65 kDa, indicating non-specific binding of the GFP and FUS antibodies. This finding was mirrored in the FUS-WT lysate there was perhaps slightly more expression than non-transgenic at the 100kDa, 75kDa and ~65kDa

mark, however this could also be due to non-specific binding. The FUS-MT lysate however showed a clear distinction between both of the other lysates, there were strong double bands just above and below the 75kDa mark and a singular strong band at approximately the ~65kDa mark that was substantially stronger than the non-specific bands located in the non-transgenic and FUS-WT lanes. Further, in this lane there were also strong bands just above the 25kDa mark, again possibly indicating fragments of the FUS-MT protein. Despite expecting the 100kDa band to be positive for FUS tagged GFP, it is evident that at 100kDa there is only non-specific binding, as the same band appeared in each lane that was run. There was a clear distinction between the protein abundance from the FUS-MT lysate compared to either of the other two lysates, and this western blot, similar to the microscopy experiments showed that the FUs-MT showed greater expression of tagged FUS than the FUS-WT line.

3.1.3. Investigating aggregation as a disease phenotype in the FUS-MT zebrafish

In a first attempt at designing experiments for high-throughput drug-testing with fast data-capture and analysis, the option of using the protein aggregates as a readout for disease state in the FUS-MT zebrafish was considered.

The first method of microscopy attempted to identify aggregates was using a screening microscope, in this case a Leica screening scope that allowed close up images. As seen in Figure 3.3 this illustrated the presence of aggregates and served to confirm the continued phenotype of aggregates within this zebrafish line. However, as seen Figure 3.3(A) there was a lot of background fluorescence seen, due to the ubiquitous nature of expression of the FUS-MT construct. This was a potential issue as attempts to quantify small point aggregates like these could become extremely difficult and error-prone due to an inability to separate the aggregates from background fluorescence using an image analysis software ImageJ (NIH). In an attempt to rectify this issue, compound imaging was carried out. Firstly, single images were taken, as seen in Figure 3.3(B), however some aggregates were getting missed due to the depth of the zebrafish larva, where aggregates could be below the field of focus in one image. Another issue with missing all the aggregates in the zebrafish larva introduced experimenter bias, whereby the experimenter taking the images is more likely to focus on the spot with most aggregates. To rectify this z-stack image with a set ‘depth’ were taken of the zebrafish larva. As seen in Figure 3.3(B) these z-stack images were much clearer however they still had some background fluorescence.

Another attempt at using microscopy to image protein aggregates as a readout for disease state utilised confocal microscopy. As seen in Figure 3.3 confocal images were much clearer than the compound or screening microscope images. There is also significantly less background fluorescence in these images. Although it is important to note that that could be because this image was taken lower down in the tail, where there was less fluorescence because the 'depth' of the tail is shallower than the 'depth' of the body of the zebrafish larva. Another note about confocal imaging is that it was much more labour intensive to prepare the zebrafish larva for confocal imaging rather than compound imaging.

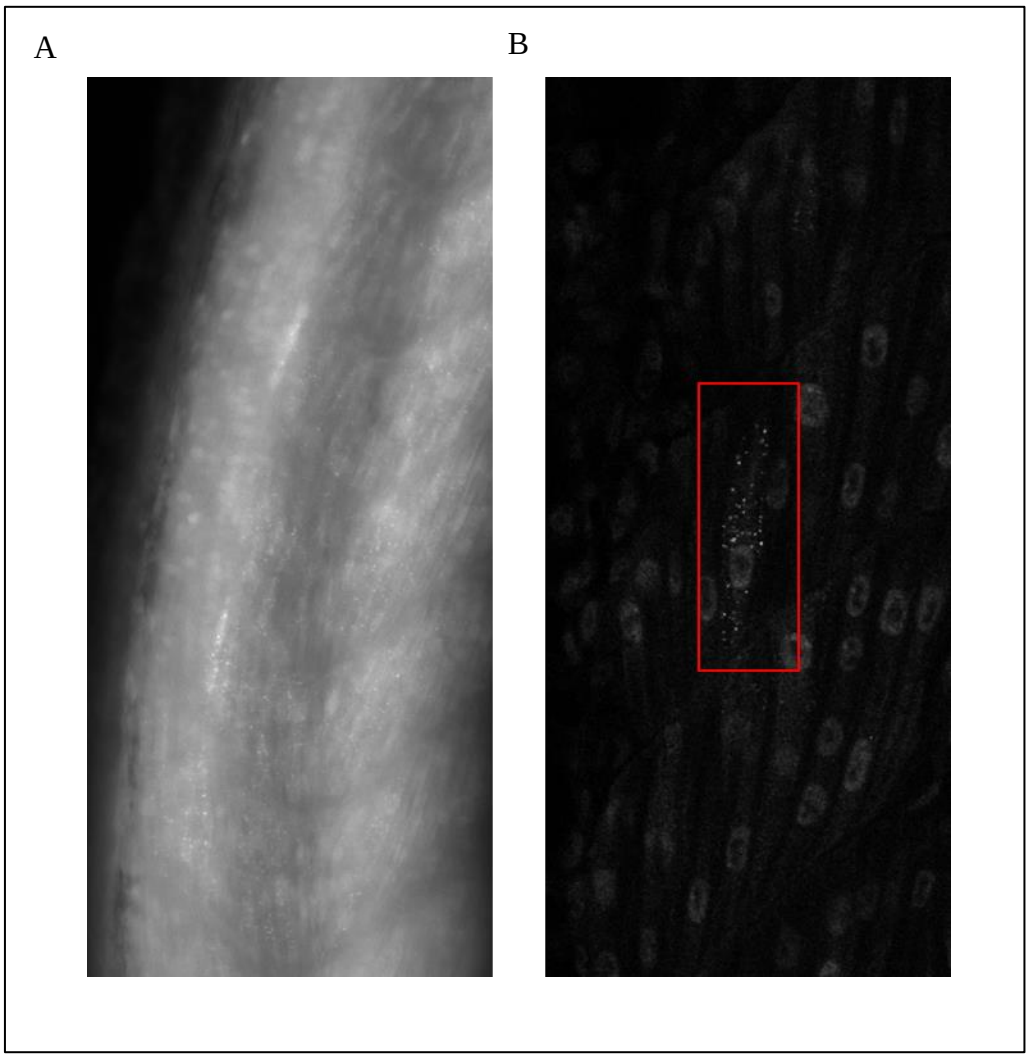

Figure 3.3. Aggregation in FUS-MT zebrafish embryos was clearer in confocal images than compound images.

(A) Z-stack composite image of 10 individual images showing the extent of the aggregation phenotype in the FUS-MT zebrafish line. Image depicts striated muscle cells in the upper spinal region of the zebrafish. Taken at 40x magnification on Leica inverted compound microscope. (B) Individual confocal image of a zebrafish larva with many aggregates. Red box indicates presence of aggregates in a single muscle cell, located in the tail of the larva. Taken at 60x magnification *using* 550 volts and 70% laser on a Leica upright SP5 confocal microscope.

When imaging the FUS-MT zebrafish it was clear that FUS protein aggregates were present within muscle cells within the zebrafish larvae. It was also investigated whether the protein aggregates were also localised within motor neurons. This was carried out by crossing the FUS-MT zebrafish line to a motor neuron reporter line (MNX:BFP) which expressed BFP in the motor neurons of the zebrafish. When imaged, if the GFP aggregates co-localised with the BFP labelled motor neurons, neuronal aggregates could be confirmed. Imaging of these MNX:BFP; actb2:Hsa.FUS_R521C-EGFP zebrafish (Figure 3.4) confirmed the presence of GFP protein aggregates within muscle cells, but protein aggreates were not easily observed within the spinal column of the zebrafish.

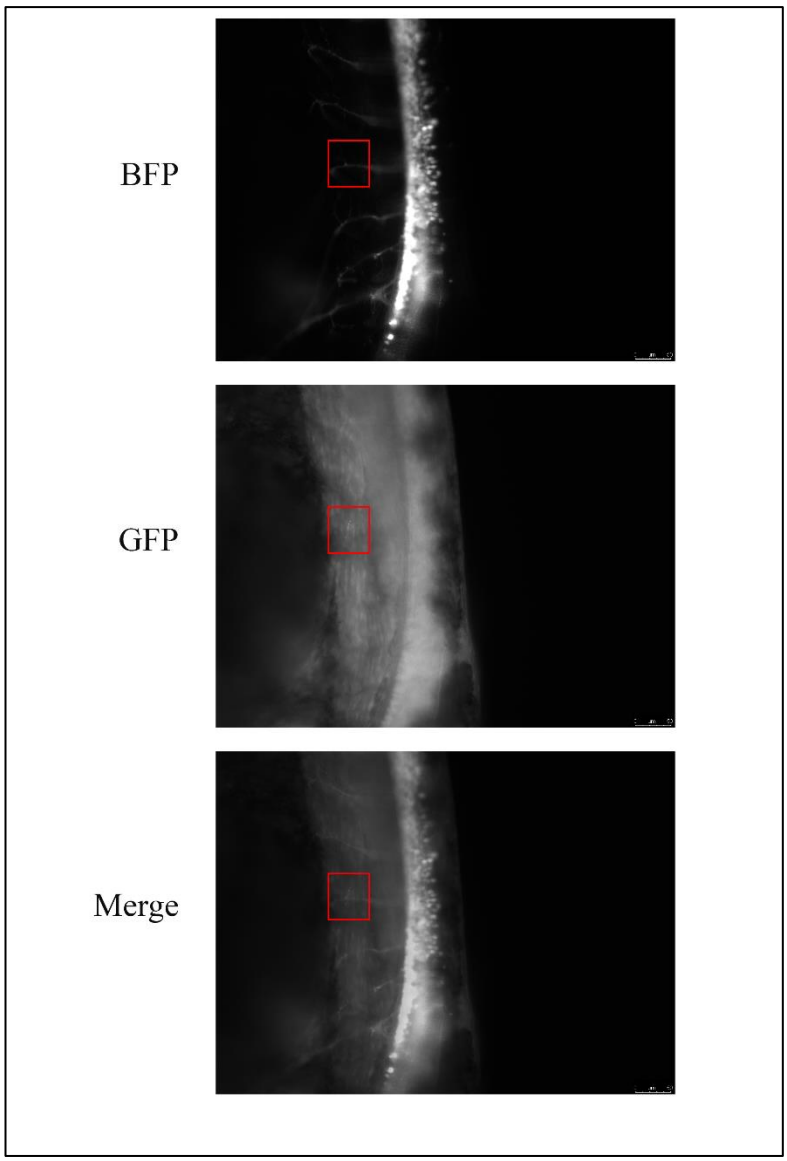

Figure 3.4. Aggregation in FUS-MT zebrafish embryos does not co-localise to the motor neurons

Images of a 2 dpf FUS-MT zebrafish embryo that was produced from an outcross between a FUS-MT and MNX-BFP setup with a limited aggregation phenotype. Scale bar is 50 µM.

While determining ideal methods to perform drug treatments on these FUS-MT zebrafish larvae, using microscopy to investigate amelioration of the aggregation phenotype was ruled out as too time consuming. This encouraged further investigation into alternative methods to investigate drug alleviation of disease phenotype.

For these reasons it was decided that microscopy was not the best method of disease readout for these zebrafish larvae, and a more important focus would be to include using western blot, cell culture or flow cytometry as a readout for whether the protein aggregation disease phenotype was ameliorated by drug treatments.

3.2. Autophagy induction visualised with western blot

Now that it had determined there was an aggregation phenotype, and a successful western blotting technique had been developed, drug testing in the zebrafish larvae could begin. For this project drug testing was achieved in two ways. The first was treating the zebrafish larvae when they were 1 dpf and adding the drug to the water. However to further the aim of this project, an attempt was made to develop the zebrafish embryos into cell culture, as a means of further developing high-throughput drug testing methods. This was carried out concurrently with 'regular' drug testing

To gain insight into the effect that inducing autophagy has on the FUS-MT zebrafish larva, drug treatments using a known autophagy inducing polyamine compound, spermidine, were carried out. A range of concentrations were tested to determine if there was a dose-dependent effect in the levels of FUS-MT protein in the zebrafish larva. All western blots were probed first for GFP first then FUS to determine if the amount of FUS-MT protein was present. Once this was confirmed the blot was probed for GAPDH as a loading control.

The western blot depicted in Figure 3.5(A) shows even loading from the GAPDH loading control in each lane of the western blot. There was a faint band seen in the non-transgenic lane, a result of non-specific binding. A decrease in FUS-MT abundance when treated with 3.125 µM and 6.25 µM spermidine is also seen in the zebrafish larva. A decrease in abundance in the top band was seen when treated with 25 µM spermidine, but not the bottom band. An increase in abundance was seen when treated with 12.5 µM and 50 µM spermidine. This trend was generally mirrored across all four replicates, as depicted through quantification in Figure 3.5(B). Quantification of FUS protein abundance saw a significant decrease with 6.25 µM spermidine treatment ($p<0.05$).

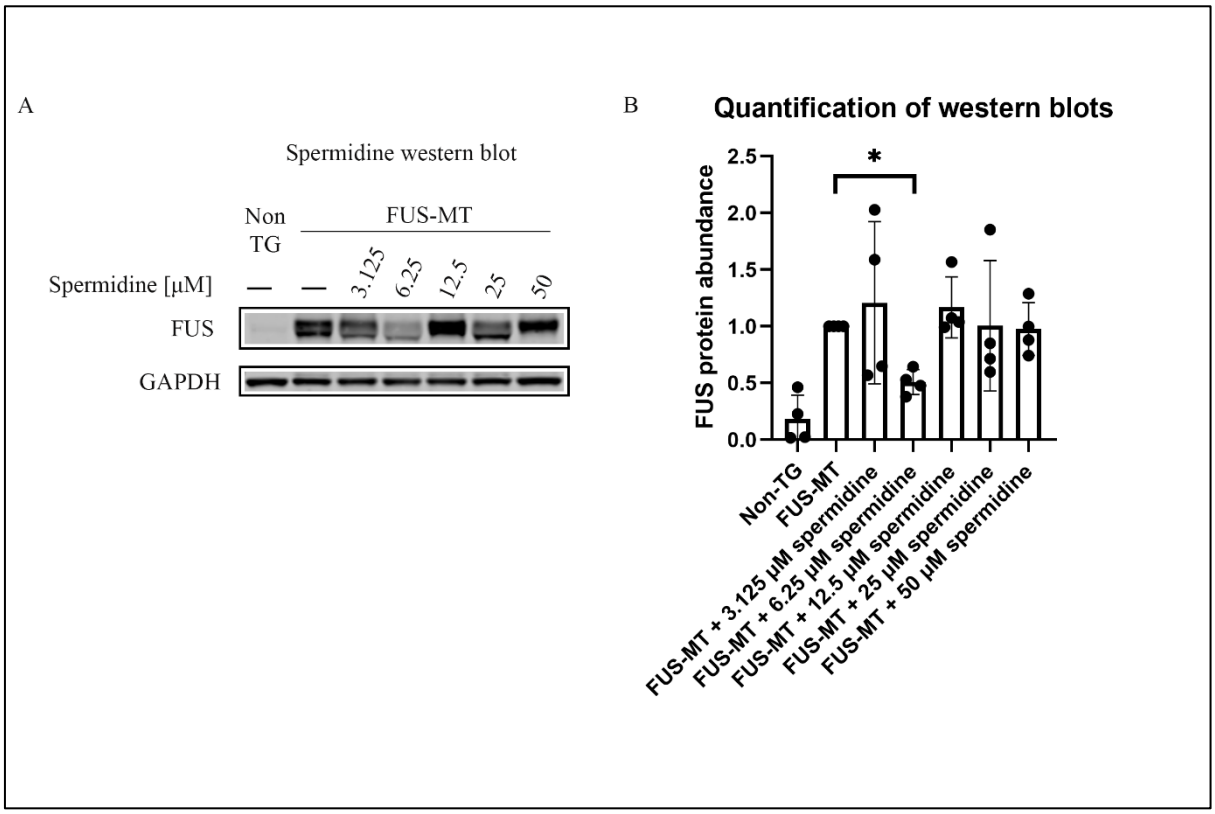

Figure 3.5. Spermidine drug treatment analysis using western blot

(A) FUS-MT zebrafish larva were treated with increasing concentrations of spermidine. Lysates were run on western blot to determine FUS protein abundance. GAPDH was used as a loading control. (B) quantification of four drug treatments completed on the FUS-MT zebrafish larva.

3.3. Zebrafish primary cell culture of FUS-MT zebrafish embryos

Zebrafish primary cell culture was attempted in order to further explore the aggregation phenoytype of the FUS-MT zebrafish line. Cell culture, if successful, may open opportunities to utilise methods such as flow cytometry and IncuCyte automated imaging, which are both high-throughput methods that still allow for drug testing. First the protocol to develop cell culture of the zebrafish larvae needed optimisation.

The first issue encountered with primary cell culture protocol was the difficulty in breaking down the zebrafish embryos completely. As shown in Figure 3.6(A) in many cases there was only partial digestion of the zebrafish embryos. Methods to improve this outcome included vigorous pipetting, longer trypsinisation times, manual removal of zebrafish tissue and an alternate digestion solution (Accumax). These had limited success. There was no difference seen between the use of Accumax or trypsin. All other methods of improving digestion also

saw a decrease in viable cells, however eventually a combination longer trypsinisation times with vigorous pipetting were used to prevent this issue.

Another issue encountered with primary cell culture was bacterial contamination. Figure 3.6(B) shows significant bacterial contamination, with very few cells. The few cells present all show morphological defects, such as roundness. To prevent bacterial contamination additional steps were added to the culturing protocol before digestion. These additional steps included incubating the zebrafish embryos (before dechorination) in Pen-Strep for 4-5 hours followed by a 2-minute wash in diluted bleach to kill any bacteria. These methods were successful in preventing bacterial contamination.

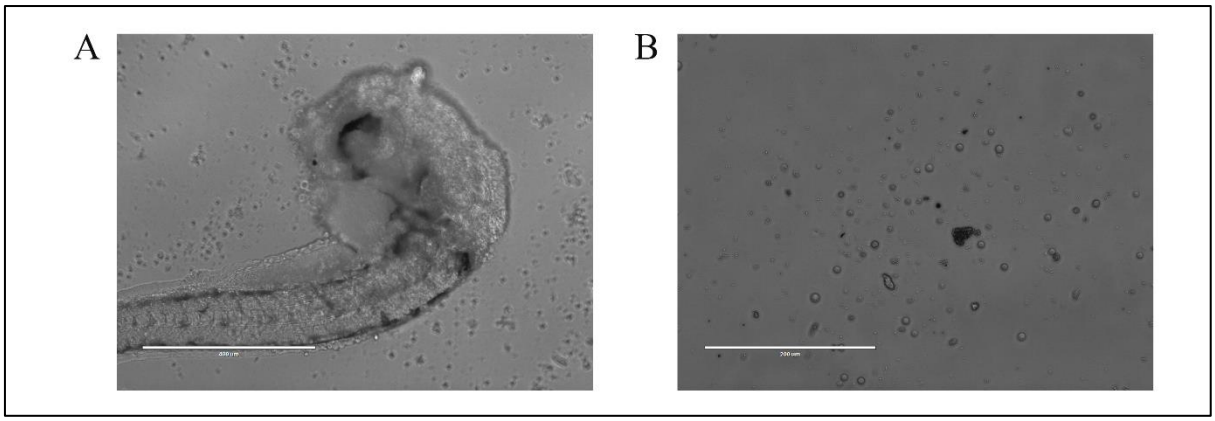

Figure 3.6. Microscopy results of cell culture optimisation techniques

(A) Image of failed trypsinisation of the zebrafish embryo in cell culture. Scale bar 400 µM. (B) Image of bacterial contamination in cell culture. Scale bar 200 µM.

3.4. Investigating fluorescence in zebrafish primary cell culture

Once the protocol for primary cell culture had been optimised, it was investigated whether the cellular pathology of the FUS-MT zebrafish larva translated into cell culture. Before directly culturing the FUS-MT zebrafish larva, another zebrafish larva line, the motor-neuron reporter line (MNX-BFP) was first chosen to culture. This was to ensure that neuronal cells were present in the final primary culture produced.

Culturing the MNX-BFP larvae was successful, and as seen in Figure 3.7 showed the presence of motor neurons in the resulting cell culture. The brightfield image also showed the presence of many neuronal processes, although the BFP expression was only seen in the cell body. This indicated there are other neuronal cell types apart from motor neurons present in the primary culture. This experiment also served to prove that fluorescence existing in the original fish was

still present in the final cell culture. This technique was then applied to the FUS-MT zebrafish line.

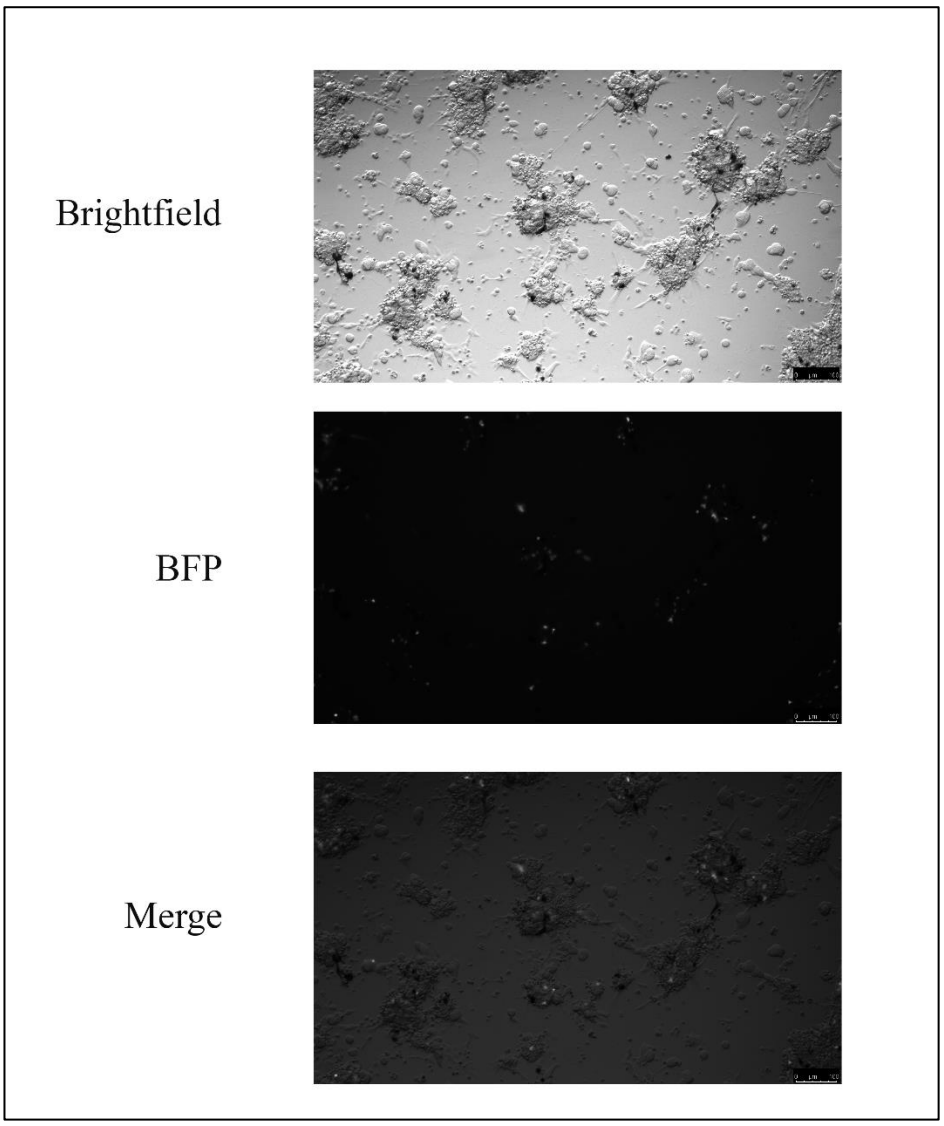

Figure 3.7. Primary culture of zebrafish MNX-BFP fish line.

Primary cell culture of MNX-BFP larvae showing BFP expression in some of the cultured cells. Scale bar 100 µM.

Unfortunately, when the primary cell culture was attempted on the FUS-MT line, the GFP expression was very faint. This is seen in Figure 3.8 where all images taken of FUS-MT culture needed very high exposure times to capture any fluorescence.

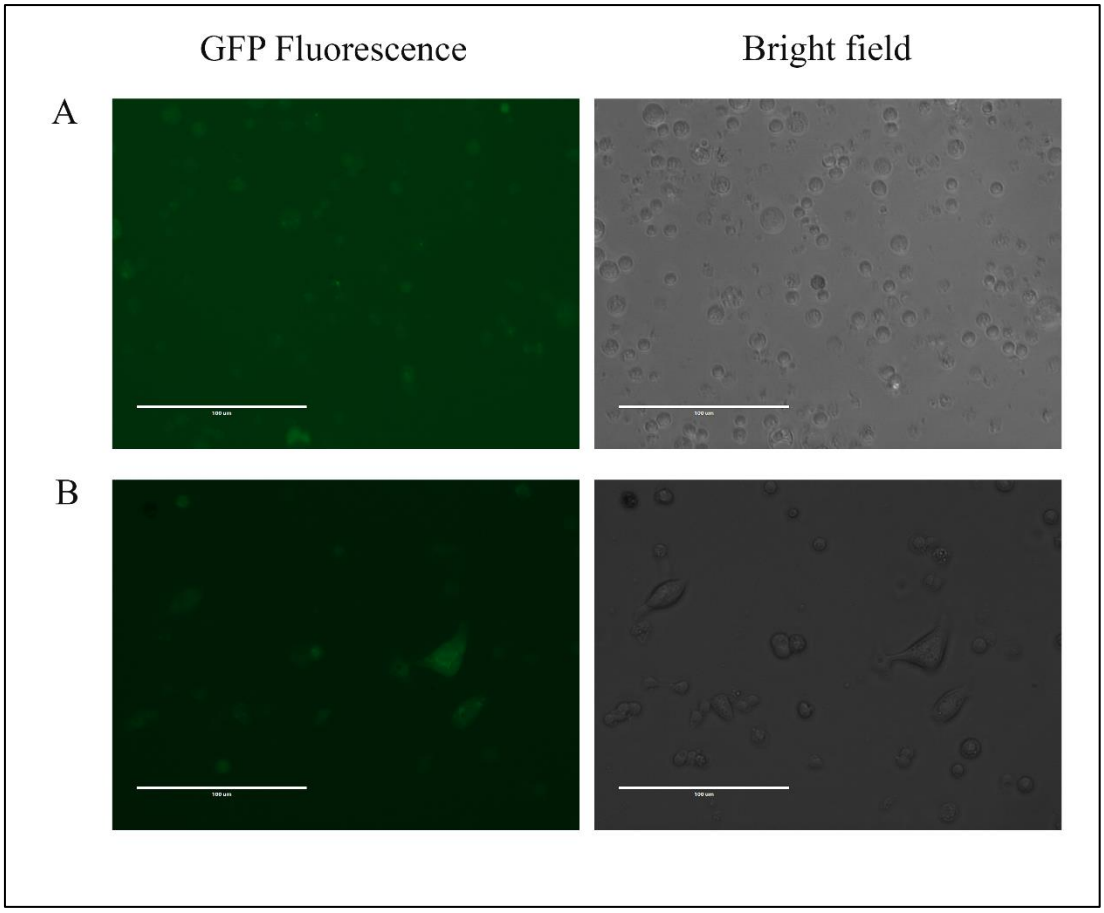

Figure 3.8. Primary cell culture of FUS-MT zebrafish larva line

(A) GFP expression seen in culture of FUS-MT zebrafish larva line. Scale bar 100 µM. (B) GFP expression seen in culture of FUS-MT zebrafish larva line. Scale bar 100 µM.

3.5. Flow cytometry of the FUSR521C zebrafish larva

The flow cytometry experiments were run on zebrafish larvae following treatment with spermidine as an autophagy inducer, and chloroquine as an autophagy inhibitor, as positive and negative controls, respectively. It was expected that spermidine would decrease the number of aggregates seen in the embryos, while chloroquine would have the opposite effect. There was a significant decrease in total aggregate particles present following treatment with 25 µM spermidine compared to untreated group ($p=0.0165$ Figure 3.9(A)). However, there was no significant difference seen between treatment with 1.5 mM chloroquine and the untreated group ($p=0.7283$). When the aggregate particles were analysed by size the same trend was seen for the smaller particles, with a significant decrease in the number of small aggregate particles present following spermidine treatment ($p=0.0346$ Figure 3.9(B)). However, when larger aggregate particles were quantified no significant difference was seen ($p=0.1960$ Figure 3.9(C)).

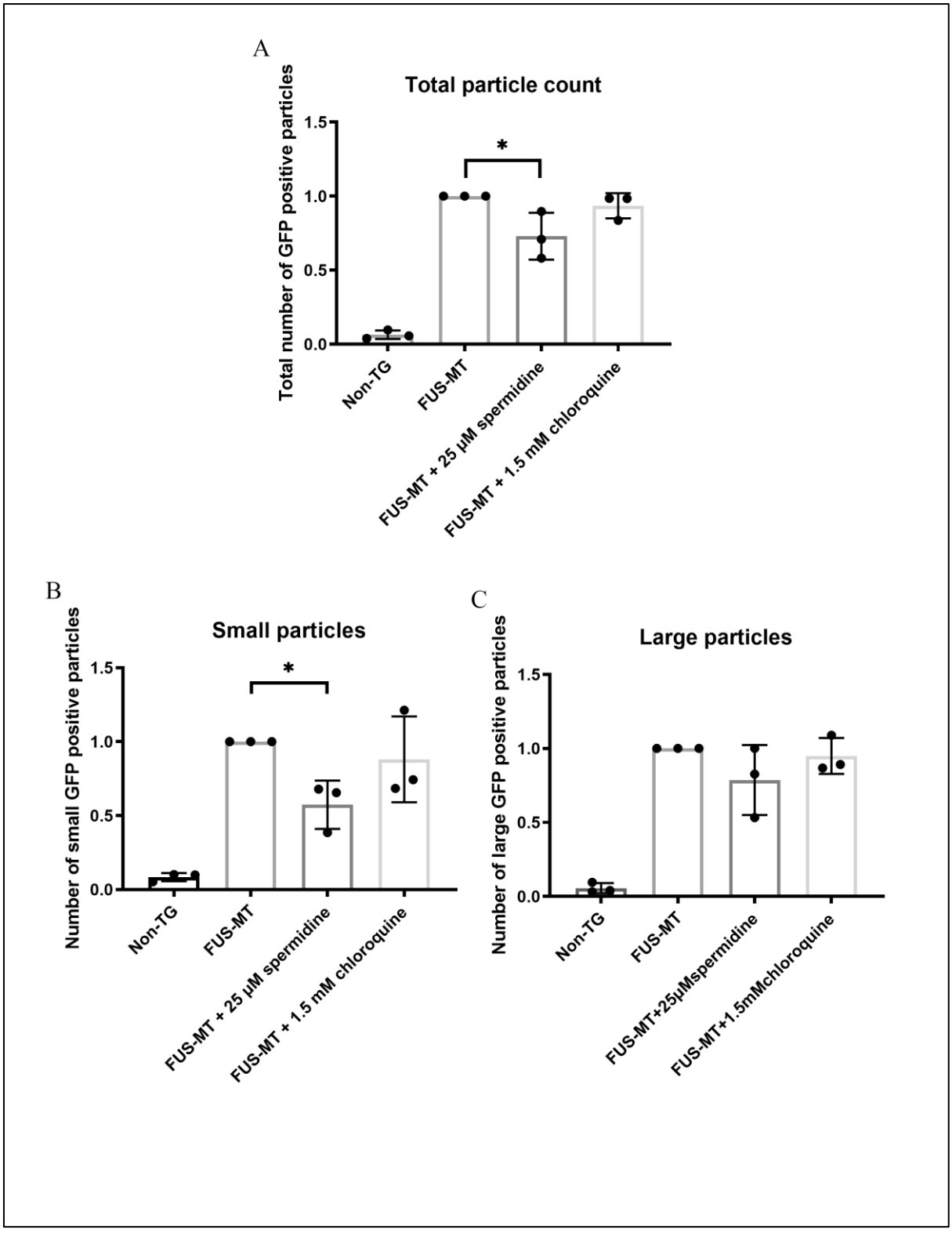

Figure 3.9. Aggregation phenotype is reduced with spermidine treatment

Flow cytometry was used to determine the extent of the aggregation phenotype in the FUS-MT larva. Gating was carried out as explained in the method section 2.8. (A) Total particle count describes the number of GFP positive particles, normalised to the number of UV positive particles for each treatment group. (B) The number of GFP positive particles, from the total number, that have a smaller FSC size than 1,000. (C) The number of GFP positive particles, from the total number, that have an FSC size greater than 1,000.

Transfection efficiency data was acquired by staining a zebrafish larvae cellular suspension (before Triton-x lysation) with Hoechst DNA live cell stain. Transfection efficiency was then calculated by quantifying the number of cells that were GFP positive expressed as a percentage of the number of cells that were UV positive. Two different methods were used to obtain the number of GFP positive cells and the number of Hoechst-stained cells. The first required taking an image of the cells, under GFP and UV fluorescence and counting the number of cells positive for each. The second method used flow cytometry to count the number of cells that fell in each spectrum within the 10,000 events. Both methods are shown below.

The transfection efficiency quantified using image analysis, as seen in Figure 3.10(A) resulted in a lower transfection efficiency than when calculated using flow cytometry (Figure 3.10(B)). This image analysis protocol for calculating transfection efficiency also produced a greater difference between the different treatment groups. In comparison, the flow cytometry transfection efficiency counting approach resulted in very similar transfection efficiency values for each of the positive MT-FUS groups. The transfection efficiency is a usefull equation, as it would allow for the application of this flow cytometry method to other transgenic zebrafish lines (that would each have different rates of fluorescent positive cells), in order to allow comparison of the amount of aggregation occurring between models.

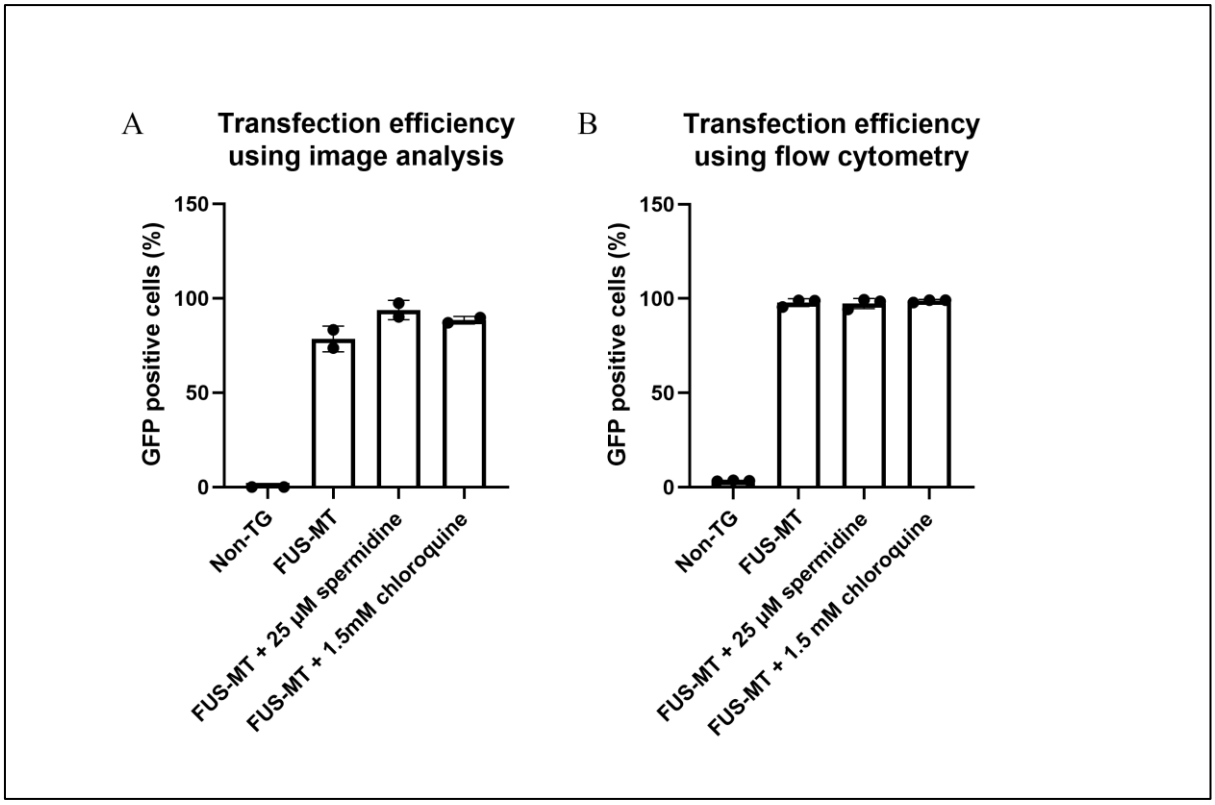

Figure 3.10. Transfection efficiency of zebrafish whole-cell suspensions using different counting methods

Microscopy or flow cytometry methods were used to calculate transfection efficiency for each treatment group of zebrafish cellular suspension. Transfection efficiency for each method was calculated by expressing the number of GFP positive cells counted over the number of Hoechst-stained cells as a percentage. (A) Transfection efficiency calculated by counting number of GFP positive cells and number of Hoechst-stained cells from microscopy images. (B) Transfection efficiency calculated by total number of GFP positive cells expressed as a percentage of total number of Hoechst-stained cells, counted using flow cytometry.

Once the trasnfection efficiency was calculated, FloIT analysis was then applied to the aggregation particle count results, in order to quantify the number of aggregates per 100 positive cells in each sample. The calculation used is as follows:

$$i = 100\left(\frac{n_i}{\gamma.\ n_{nuc}}\right)$$

where n_i is the number of inclusions present, n_{nuc} is the number of nuclei present, and γ is the transfection efficiency.

The FloIT aggregate analysis calculation revealed a significant decrease, as seen in Figure 3.11 in the number of GFP positive particle aggregates per 100 fluorescent cells, following treatment with spermidine ($p=0.286$) There was no significant difference between the aggregate count with chloroquine treatment and untreated controls ($p=0.5921$).

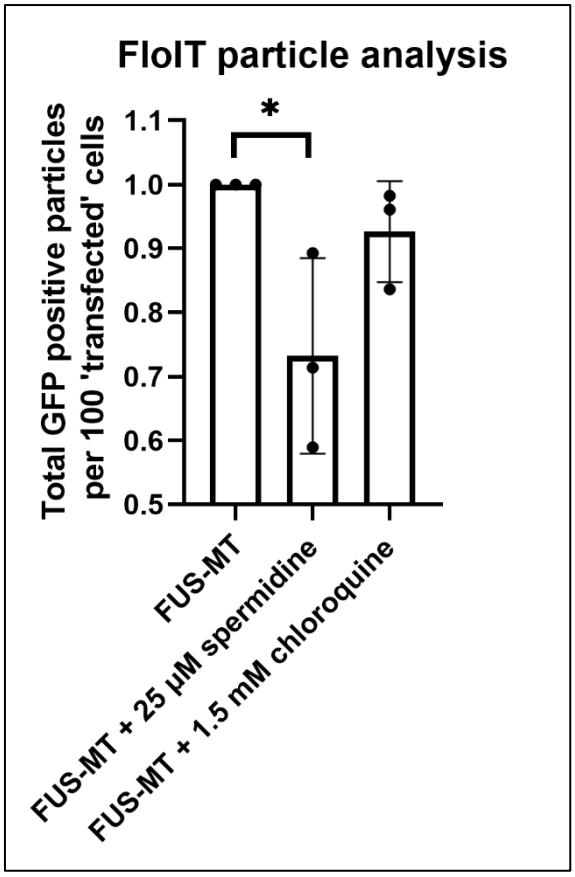

Figure 3.11. Aggregation phenotype is reduced by treatment with spermidine

FloIT analysis applied to total aggregate particle count using the transfection efficiency values that were calculated using flow cytometry. Non-transgenic group was excluded as explained in methods section 2.11.

4. Discussion

4.1. Characterisation of transgenic mutant human FUS Zebrafish line

The first aim of this project was to further characterise the mutant human FUS (R521C-GFP, FUS-MT) and wildtype human FUS (WT-GFP, FUS-WT) transgenic lines for pathophysiological traits. These lines had already been previously characterised for pathophysiological characteristics and the FUS-MT line was found to carry stress granules, with both wildtype and mutant FUS transgenic zebrafish lines expressing strong fluorescence throughout the zebrafish (Acosta et al., 2014). However, before beginning experimentation it was important to ascertain whether characteristics of the trangenic lines had changed within successive generations of these zebrafish lines. Silencing can often occur in transgenic zebrafish lines over time, resulting in a loss of fluorescence from either silencing of just the GFP tag or the actual protein itself (Goll, Anderson, Stainier, Spradling, & Halpern, 2009). Therefore characterising these transgenic zebrafish began with determining relative fluorescence levels between the FUS-MT and FUS-WT (FUS-WT) lines.

Having both lines available for experiments is important, as the FUS-WT line can act as a negative control, to easily demonstrate what is occurring in the FUS-MT line is due only to the effect of the protein mutation expressed throughout the zebrafish. For this reason it would be ideal for the FUS-WT line to have FUS expression levels equal to or greater than the FUS-MT line. Another important negative control when using zebrafish embryos can be use of negative siblings of the transgenic line, as these zebrafish have a similar genetic background as their positive siblings, however they are simply lacking the transgenic construct. In this case, negative siblings can be obtained if an outcross is made between adult zebrafish of the transgenic line to a non-transgenic line, such as WT-TAB (non-transgenic). Thus, the first experiment to compare and contrast relative GFP expression level in different transgenic lines using microscopy was carried out.

As seen in Figure 3.1(A) it was found that the FUS-WT zebrafish line had limited to no fluorescent expression, compared to the FUS-MT line, which had strong expression levels. This result was further confirmed via western blot displayed in Figure 3.2. Unfortunately this meant that the FUS-WT line was unable to be used in the remaining experiments, until the line was re-derived. However, as shown in Figure 3.1(B), the FUS-MT line was able to produce

negative siblings, which, while not the perfect control group, could be used in the drug treatment studies as a reference group. Otherwise, another choice of negative control for drug treatment studies is simply using non-transgenic controls, as this line would also lack the mutated human protein. Nevertheless, the most important control group for drug treatment studies is a 'untreated control' which, in this case, would be the FUS-MT larvae without having a drug applied.

4.2. Microscopy investigation into protein aggregation

An important facet of MND progression in humans is the accumulation of aggregates within motor-neurons. This is also true for familial FUS mutations, wherein FUS-positive protein aggregates have been reported to be present in both patient autopsy samples and neurons derived from patient induced pluripotent stem cells (Marrone et al., 2019). Although it is still unclear whether aggregates are a direct cause of the progression of MND or simply a by-product of the disease, they have a clear connection to the disease. One finding that studied a mouse SOD1 aggregation model found that the areas least affected by the disease had the most aggregation (Gill et al., 2019). The FUS-MT zebrafish line used in this study was previously reported to have an aggregation phenotype, but before new experiments could begin this needed to be re-confirmed (Acosta et al., 2014). As well as this, an aggregation phenotype could potentially be used as a readout for the disease progression as if fewer aggregates are seen after a drug treatment, then that could be a sign the drug is having an effect. For this reason, microscopy methods were used to investigate the aggregation phenotype of FUS-MT zebrafish larvae.

Confocal and compound microscopy were both considered as tools to further investigate the effect drug treatments may have on the aggregation phenotype, using *in vivo* imaging. Z-stack imaging is essential for this research and unfortunately screening fluorescence microscopes do not allow the aggregate images to be seen clearly due to their lower magnification. Both confocal and compound microscopy revealed a significant aggregation phenotype in the FUS-MT larva. However, it was expected that no aggregates would be seen in the motor neurons of the zebrafish larva, as when taking the Z-stack images, located near the spine, aggregates were only seen in the muscle cells, not in the spinal cord. Figure 3.4 demonstates this previous finding which shows the aggregates present in this zebrafish larva are located in muscle cells, and not the motor neurons of the imaged zebrafish larva.

The MND disease progression in humans occurs in the motor neurons leading to the brief probe to determine whether the FUS-MT larva aggregate expression occured in the motor neurons. This was achieved by a cross with the FUS-MT line with a reporter line (MNX-BFP) that expresses blue fluorescent protein solely in the motor neurons of the larva. The results were shown in Figure 3.3, which showed frequent protein aggregates within muscle cells. Whilst protein aggregates were not easily observed within motor neurons within this study, they were previously reported to be present within motor neurons within this zebrafish line (Acosta et al., 2014).

The images derived from compound and confocal microscopy, Figure 3.3(A) and Figure 3.3(B) respectively, are taken in different areas of the zebrafish larvae, however the quality of the pictures is clear from an image analysis standpoint. Using a confocal microscope shows much less of the background GFP, caused by ubiquitous overexpression of the mutated protein, to permeate the image. The aggregates within these imaged zebrafish larvae was clearer, which made it easier for the thresholding function within image analysis software (e.g. Image J from NIH) to analyse and count the number of aggregates within each of the images. The excess background in the original compound images lead to many false positives to be counted, with the image analysis software counting aggregates where there were none. Using clearer confocal images would hopefully mean less false positives leading to more confidence in the results. However the time taken to capture each image must also be taken into account. The set-up required to image larvae under a confocal microscope, is far greater than compound microscopy as detailed in methods section 2.11. Although possibly the most reliable method, microscopy is unfortuantely a time consuming process, and in order to potentially develop high-throughput drug testing methods to interrogate drugs that would ameliorate the aggregation phenotype of this FUS-MT strain, other methods such as primary culture were considered.

4.3. Drug testing studies using western blot to measure protein expression

One of the purposes animal disease models fulfill, is to be used for drug treatment studies, to determine if a drug might be a possible candidate for use in human patients. Drug treatments are a relatively simple process with zebrafish, as drugs can be added directly to the media the zebrafish are kept in where they are then absorbed by the zebrafish larvae. Western blotting

can then be used to interrogate protein samples generated from drug treated larva to determine whether the drug has had an effect on the abundance of the mutated protein in question, in this case mutated huam FUS-GFP. Drug testing in this project focused on testing spermidine, a previously reported autophagy inducer, that has had positive findings in other zebrafish disease model testing (unpublished data, Maxinne Watchon PhD thesis). It was hypothesised that stimulating the autophagy protein quality control pathway would reduce the abundance of FUS-MT protein. Spermidine has previously been shown to alleviae motor symptoms in a TDP-43 mouse model, through induction of the autophagy pathway in an MTOR-independent manner (I.-F. Wang, Tsai, & Shen, 2013). This model was also used to test other drugs such as resveratrol, which functioned in an MTOR-dependent mannor, producing similar results (I.-F. Wang et al., 2012).

The western blotting investigation into the effect of spermidine treatment on levels of human FUS protein in the FUS-MT zebrafish larvae revealed a significant reduction of human FUS-GFP protein at the 6 µM treatment concentration. However, other concentrations, above and below 6 µM had no significant effect on human FUS-GFP protein levels. This was in contrast with initial expectations as previous work in zebrafish revealed the ideal concentration for autophagy induction was 25 µM (Mathai et al., 2017). Western blotting is a valuable method that can reveal detailed information about abundance levels of multiple proteins at once. In future experiments, this method should also be used to investigate levels of autophagic proteins such as LC3B and p62/ Sequestosome-1, which can be used to determine if autophagy has been induced. Proving that the spermidine treatment had caused the induction of autophagy is necessary as this would provide further evidence that autophagy enhancers are potential ideal candidattes to test in models of MND.

Future investigations into protein levels of autophagy markers and substrates using this model would need to take into consideration that the original banding revealed in Figure 3.2 showed multiple bands between 60 and 100 kDa. These present difficulties when probing for a commonly used autophagy marker, p62 because probing for p62 would have to occur first before probing for FUS or GFP in each replicate western blot membrane, to prevent the multiple bands seen when the membrane was probed for FUS and GFP antibodies.

Despite the reliable nature of western blot analysis, in an attempt to develop a more high-throughput drug screening method primary cell culture was explored.

4.4. Cell culture as a method to investigate protein aggregation

Primary cell culture of FUS-MT larvae was then attempted, in order to further investigate the aggregation phenotype of the cells. The original protocol used manual dechorination using sharp forceps, before washing embryos in sterile media, euthanasia, trypsinisation then plating the resultant cell suspension. This worked to an extent, however as seen in Figure 3.5, there were issues encountered including massive bacterial contamination and failure to dissolve the main body of the zebrafish larvae. The resultant bacterial contamination can be attributed to non-sterile procedures such as manual dechorination, despite using sterile media later in the protocol.

Fixing the bacterial contamination was a simple solution that aimed to keep the embryos in a more sterile environment throughout the process. This required a five-hour incubation in a strong solution of penicillin and streptomycin (Pen-Strep) in E3, followed by a two-minute bleach wash then sterile dechorination using Proteinase K. This prevented any bacterial contamination from being seen, however it also increased the time required for carrying out this protocol, which, it could be argued, negated the aim of developing high throughput methods for drug testing. Using antibiotics in cell culture should also be undertaken with caution, as one study found that Pen-Strep affected gene expression of ~200 genes, including transcription factors (Ryu, Eckalbar, Kreimer, Yosef, & Ahituv, 2017). Although other primary embryonic zebrafish cell culture protocols deem antibiotics a necessity (Sassen et al., 2017).

Another major issue encountered with this protocol was the inability for trypsin to completely dissolve the body of the zebrafish embryos. One attempt to remove the zebrafish tissue from the cellular mixture was to remove them manually, by pipetting them out. However, this was difficult to achieve and led to a reduced number of viable cells that had already been dissociated, resulting in fewer cells available to be plated. Another attempt to rectify this included pipetting more vigorously in order to further break up the embryos manually, which worked to an extent, but also caused more cellular damage and debris with cells that acquired poor morphology. The pipetting also needed to be performed in a sterile manner, to prevent bacterial contamination of the sample, was carried out inside a sterile biological safety cabinet. However, the continuous switching between the heated water bath and sterile biosafety also increased the time taken to carry out the protocol. This effect was compounded when another method attempted included longer trypsinisation times up to 45-60 minutes, from initial times of only 5-15 minutes, although this method worked well. A compromise between these two

methods, including longer trypsinisation with occasional pipetting, in a sterile manner was used to successfully grow primary cultures of zebrafish larvae.

Despite the current obstacles to preforming this protocol, future optimisation could see this as a useful protocol. Future optimisation should address the difficult digestion of the zebrafish tissue. Other studies have noted that the digest is improved with a cocktail of digestion enzymes consisting of collagenase, proteinase K, trypsin and hyaluronidase (Gallardo & Behra, 2013). collagenase and hyaluronidase were strategically chosen to target the difficult to break down conjunctive tissues of the larvae mainly consisting of the extracellular matrix (ECM), of which collagen and hyaluronan are the main components (Gallardo & Behra, 2013). Proteinase K was also included to inactivate DNAses and RNAses, as well as increase permeabilization of tissues (Gallardo & Behra, 2013). Although other protocols have streamlined this process and used only Collagenase and trypsin (Bresciani, Broadbridge, & Liu, 2018). Future optimisation should also include using a 40 µM strainer. This would allow manual removal of any left-over particulates by passing the primary zebrafish cell suspension through the strainer. This would minimise the loss of viable cells and cell counting and plating could then follow normally.

The next issue with the cells was a lack of fluorescence. After the first attempt at plating out cells from the FUS-MT zebrafish larvae and seeing no fluorescence a replicate using the MNX-BFP zebrafish was attempted. This went somewhat better with BFP being spotted using a Leica inverted compound microscope, this also allowed for the identification of motor neurons in the plated cells. Once this was achieved the protocol was repeated with the FUS-MT zebrafish, however, as seen in Figure 3.8, there was still limited fluorescence. Indeed, it was difficult to see fluorescence in these cells without using a very high exposure time to capture images. One hypothesis behind the lack of fluorescence seen could be due to cell death or loss of cells during the culturing process. Other studies that cultured primary zebrafish cells have had no issue with fluorescence intensity (Sassen et al., 2017). One of the original intentions behind developing primary cell culture, was to analyse the aggregation phenotype using a multi-well cell imaging device, such as the IncuCyte. However, the low fluorescence prevented this. At this point the lack of fluorescence and the time-consuming nature of the method prevented continued optimisation of this protocol.

Other potential methods that could have been chosen include using existing immortal cell culture methods, rather than primary culture, such as human HEK cells or neural cells such as

the mouse line NSC-34 (Madji Hounoum et al., 2016; Thomas & Smart, 2005). A potential disadvantage of using immortal cell culture models is the increased risk of cross-contamination, commonly with HeLa cells, that have the ability over several passages of cell to replace the existing cell line entirely (Kaur & Dufour, 2012). However there are distinct advantages to using immortal cell lines including ethical considerations and cost effectiveness furthermore one study suggests that the risk of cross-contamination can be remedied or removed by performing authentication testing on cell lines used (Capes-Davis et al., 2010). However, for this research purpose, using an immortal cell line would require developing a stable FUS transgenic cell culture line, which would arguably require more resources to complete, as currently only transient cell culture models are used within our team.

Alternatively, stable cell culture lines of transgenic zebrafish could be used (Ciarlo & Zon, 2016). This technique is less frequently used, in part due to their unknown genetic and physiological characteristics as these cell lines have remained relatively uncharacterised (Chen, Burgess, Golling, Amsterdam, & Hopkins, 2002; Driever & Rangini, 1993; He et al., 2006). These immortalised zebrafish cell lines also tend to focus on cell types that are not directly relevant to neuronal research (Chen et al., 2002). Ideally motor neuron cell cultures would be used in order to study MND and while these are valuable techniques, secondary cultures are not currently available and using them would not have allowed investigation into the disease phenotypes already present in the FUS-MT zebrafish.

Should optimisation of the protocol used in this project be undertaken in the future, efforts should focus primarily on reducing the amount of time it takes to complete this protocol. The primary reason this protocol was discontinued mid-way through optimisation was the excessive amount of time taken to complete each round of treatment, cell culture and quantification. At this point of the project, considering the overall aim was to develop high-throughput methods in which to carry out drug testing, it was decided to discontinue optimising the primary cell culture. Fortunately, it was realised that using the flow cytometer didn't necessarily require the cells to first be cultured. A new method was thus developed to use the flow cytometer to measure the aggregation phenotype, instead of first generating primary cell cultures.

4.5. Flow cytometry as a method of investigating protein aggregation

For the reasons described above primary cell culture of FUS-MT zebrafish larva was discontinued. Instead, in order to measure the aggregation phenotype present in the FUS-MT line, a new method was developed in order to run flow cytometry on the FUS-MT zebrafish larvae. This method still required dissolving the embryos using trypsin, however instead of using the dissociated cell suspension to first cultivate neuronally enriched primary cell cultures, they were instead run straight through the flow cytometer. This method worked well in comparison to the tandem cell culture-flow cytometry approach.

This method still had issues with zebrafish larva tissue not dissociating when using trypsin. However as part of routine use of the flow cytometer, a 40 µM strainer is used when running each flow cytometry sample, this was able to remove the clumped matter from the sample solution. This method was also not carried out in a sterile manner, which made regular pipetting an easier experience, compared with the primary cell culture procedure. Thus this protocol was found to be more high-throughput than the primary cell culture, while still having the ability to perform drug treatments. Drug treatments for these experiments were carried out in the same manner as for western blotting, except instead of making protein lysates at the end stage, a cell suspension was made instead. Drug treatments on the FUS-MT larvae were performed using spermidine (autophagy inducer) and chloroquine (autophagy inhibitor) with the expectation that spermidine would decrease the number of aggregates seen while chloroquine would increase the number of aggregates (Mauthe et al., 2018).

When choosing an appropriate concentration of spermidine to test using flow cytometry, the western blotting results were initially considered. As previously discussed a significant decrease was only seen when the FUS-MT zebrafish were treated with 6.25 µM spermidine, despite expecting the 25 µM concentration to exhibit a greater effect in protein reduction. However previously published investigation of autophagy induction in zebrafish showed that the ideal concentration used to induce autophagy in zebrafish larvae was 25 µM (Klionsky et al., 2016). Thus, for initial flow cytometry experiments, the spermidine concentration used was 25 µM. However, for future experiments, as in the previous western blot experiments, other concentrations of spermidine should be tested in order to compare and contrast to results seen in the western blot experiments. Similarly for chloroquine, the recommended dosage for

zebrafish autophagy inhibition was 3 mM however a lower concentration of 1.5 mM was selected for initial testing, although future experiments should test using 3 mM concentration (Klionsky et al., 2016). With concentrations chosen, drug testing on the FUS-MT zebrafish larvae began.

Flow cytometry results revealed a significant decrease in the total particle count when the FUS-MT larvae were treated with spermidine, indicating that when autophagy is induced, less aggregates are seen. This trend was also seen when small particles were analysed, but not large particles. There was also no significant difference seen when chloroquine was added, although this is possibly because a lower concentration 1.5 mM rather than the recommended 3 mM was used. No difference was seen in the number of large particles between any of the FUS-MT groups. In each category there was a low false positive discovery rate seen in the non-transgenic groups. Future experiments should test higher concentrations of chloroquine to determine if there is a significant increase in aggregation, as this would provide more evidence that suggests autophagy inducers are good potential drug candidates for MND.

The flow cytometry methods used to quantify aggregation in zebrafish embryos were based heavily on methods developed previously (Whiten et al., 2016). However these methods were developed based on cell culture models. In order to compare aggregate count between samples, (Whiten et al., 2016) used transfection efficiency (counting the number of transfected cells) to determine aggregate count/cell. This method doesn't quite apply in this *in vivo* setting because transfection efficiency does not exist in a zebrafish model. For example, in this FUS zebrafish model the fluorescence is ubiquitous throughout the zebrafish larva (Figure 3.1). Furthermore as seen in Figure 3.3 the aggregation phenotype demonstrates that there are fewer cells displaying the aggregation phenotype, but often when they do, there are multiple aggregates per cell. However in order to fully explore the differences between conducting these experiments in cell culture and zebrafish, an approximation was needed for transfection efficiency, otherwised described as a rate of 'GFP positive cells'. Transfection efficiency was calculated in two ways as demonstrated in Figure 3.10. These methods included image analysis consisting of manually counting the number of GFP and Hoechst-stained cells in images, and using flow cytometry methods to count GFP and Hoeschst-stained cells, and these methods were compared to determine which method was superior. It was found that the flow cytometry method was more efficient and reliable in contrast to the image analysis method. The transection efficiency values determined using flow cytometry were all very similar, compared

to slightly more variance in values seen in the image analysis. FloIT aggregagte analysis could then be applied using the total particle count to determine how many aggregates were found in each sample, taking transfetion efficiency into account.

The FloIT analysis as seen in Figure 3.11 was able to demonstrate that there were less aggregates found when the FUS-MT fish were treaed with spermidine, further validating the original finding in Figure 3.9A. There was one disadvantage when applying FloIT analysis to the total particle count. The FloIT analysis technique could not be applied to the non-transgenic group, hence that group was excluded from Figure 3.11, as there were still (albeit few) GFP positive particles seen ($n_i>0$), and the transfection efficiency was greater than zero ($\gamma>0$), which when entered into the equation, would falsely show there were even more aggregates than in the FUS-MT larva. This could have been mitigated if the image-calculated transfection efficiency had been used for FloIT calculations, as the transfection efficiency calculated for non-transgenic was then 0. However the more accurate flow cytometry analysis transfection efficiency values were used, leading to the exclusion of the non-transgenic group for FloIT analysis. The FloIT analysis is an excellent analysis technique as it could allow standardisation between results from different zebrafish aggregation models for comparison.

4.6. Conclusion

In order to develop drug testing methods for application to the transgenic FUS zebrafish model this project explored various approaches. This included a brief comparison between microscopy methods, which found both to be accurate and reliable however, did not have the capacity for high throughput drug testing or potential large scale application. In order to further explore the aggregation phenotype of the FUS-MT zebrafish, *in vitro* primary cell culture was also investigated. This method, had it functioned perfectly, would have been in an ideal position to further both high-throughput drug testing and produced comprehensive results on the aggregation phenotype. However, if in the future this method could improve the strength of the fluorescent signal seen in primary cell culture of the zebrafish larva, then there is potential to use this method for high-throughput drug testing.

As a final conclusion, the flow cytometry results seen in this project, present an exciting opportunity, while not found to be extremely high throughput, they remain, as the microscopy experiments do, a thorough and reliable method to investigate aggregation in the FUS-MT zebrafish line. Using the flow cytometry method it was possible to identify that treating the

mutant FUS zebrafish with spermidine reduced the number of FUS protein aggregates which warrants further investiatin into autophagy inducers for the treatment of MND.

References

Acosta, Jamie R, Watchon, M., Yuan, K. C., Fifita, J. A., Svahn, A. J., Don, E. K., … Laird, A. S. (2018). Neuronal cell culture from transgenic zebrafish models of neurodegenerative disease. *Biology Open*, *7*(10), bio036475. https://doi.org/10.1242/bio.036475

Acosta, Jamie Rae, Goldsbury, C., Winnick, C., Badrock, A. P., Fraser, S. T., Laird, A. S., … Cole, N. J. (2014). Mutant Human FUS Is Ubiquitously Mislocalized and Generates Persistent Stress Granules in Primary Cultured Transgenic Zebrafish Cells (E. J. Coulson, Ed.). *PLoS ONE*, Vol. 9. https://doi.org/10.1371/journal.pone.0090572

Andersen, S. S. L. (2001). Preparation of dissociated Zebrafish spinal neuron cultures. *Methods in Cell Science*, *23*(4), 205–209. https://doi.org/10.1023/A:1016349232389

Bjørkøy, G., Lamark, T., Pankiv, S., Øvervatn, A., Brech, A., & Johansen, T. B. T.-M. in E. (2009). Chapter 12 Monitoring Autophagic Degradation of p62/SQSTM1. In *Autophagy in Mammalian Systems, Part B* (Vol. 452, pp. 181–197). https://doi.org/https://doi.org/10.1016/S0076-6879(08)03612-4

Bonafede, R., & Mariotti, R. (2017). MND Pathogenesis and Therapeutic Approaches: The Role of Mesenchymal Stem Cells and Extracellular Vesicles. *Frontiers in Cellular Neuroscience*, *11*, 80. https://doi.org/10.3389/fncel.2017.00080

Bosco, D. A., Lemay, N., Ko, H. K., Zhou, H., Burke, C., Kwiatkowski Jr, T. J., … Hayward, L. J. (2010). Mutant FUS proteins that cause amyotrophic lateral sclerosis incorporate into stress granules. *Human Molecular Genetics*, *19*(21), 4160–4175. https://doi.org/10.1093/hmg/ddq335

Bradford, Y. M., Toro, S., Ramachandran, S., Ruzicka, L., Howe, D. G., Eagle, A., … Westerfield, M. (2017). Zebrafish Models of Human Disease: Gaining Insight into Human Disease at ZFIN. *ILAR Journal*, *58*(1), 4–16. https://doi.org/10.1093/ilar/ilw040

Bresciani, E., Broadbridge, E., & Liu, P. P. (2018). An efficient dissociation protocol for generation of single cell suspension from zebrafish embryos and larvae. *MethodsX*, *5*, 1287–1290. https://doi.org/10.1016/j.mex.2018.10.009

Capes-Davis, A., Theodosopoulos, G., Atkin, I., Drexler, H. G., Kohara, A., MacLeod, R. A. F., … Freshney, R. I. (2010). Check your cultures! A list of cross-contaminated or misidentified cell lines. *International Journal of Cancer*, *127*(1), 1–8. https://doi.org/10.1002/ijc.25242

Chen, W., Burgess, S., Golling, G., Amsterdam, A., & Hopkins, N. (2002). High-Throughput Selection of Retrovirus Producer Cell Lines Leads to Markedly Improved Efficiency of Germ Line-Transmissible Insertions in Zebra Fish. *Journal of Virology*, *76*(5), 2192 LP – 2198. https://doi.org/10.1128/jvi.76.5.2192-2198.2002

Chiò, A., Mazzini, L., D'Alfonso, S., Corrado, L., Canosa, A., Moglia, C., … Al-Chalabi, A. (2018). The multistep hypothesis of MND revisited: The role of genetic mutations. *Neurology*, *91*(7), e635–e642. https://doi.org/10.1212/WNL.0000000000005996

Ciarlo, C. A., & Zon, L. I. (2016). Chapter 1 - Embryonic cell culture in zebrafish. In H. W.

Detrich, M. Westerfield, & L. I. B. T.-M. in C. B. Zon (Eds.), *The Zebrafish* (Vol. 133, pp. 1–10). https://doi.org/https://doi.org/10.1016/bs.mcb.2016.02.010

Collodi, P. (2004). A Unique Journal for a Unique Experimental Model. *Zebrafish*, *1*(1), 1. https://doi.org/10.1089/154585404774101608

Deng, H.-X., Zhai, H., Bigio, E. H., Yan, J., Fecto, F., Ajroud, K., … Siddique, T. (2010). FUS-immunoreactive inclusions are a common feature in sporadic and non-SOD1 familial amyotrophic lateral sclerosis. *Annals of Neurology*, *67*(6), 739–748. https://doi.org/10.1002/ana.22051

Dharmadasa, T., & Kiernan, M. C. (2018). Riluzole, disease stage and survival in MND. *The Lancet Neurology*, *17*(5), 385–386. https://doi.org/10.1016/S1474-4422(18)30091-7

Driever, W., & Rangini, Z. (1993). Characterization of a cell line derived from zebrafish (brachydanio rerio) embryos. *In Vitro Cellular & Developmental Biology - Animal*, *29*(9), 749. https://doi.org/10.1007/BF02631432

Eisenberg, T., Knauer, H., Schauer, A., Büttner, S., Ruckenstuhl, C., Carmona-Gutierrez, D., … Madeo, F. (2009). Induction of autophagy by spermidine promotes longevity. *Nature Cell Biology*, *11*(11), 1305–1314. https://doi.org/10.1038/ncb1975

Fujita, Y., & Okamoto, K. (2005). Golgi apparatus of the motor neurons in patients with amyotrophic lateral sclerosis and in mice models of amyotrophic lateral sclerosis. *Neuropathology*, *25*(4), 388–394. https://doi.org/10.1111/j.1440-1789.2005.00616.x

Gallardo, V. E., & Behra, M. (2013). Fluorescent activated cell sorting (FACS) combined with gene expression microarrays for transcription enrichment profiling of zebrafish lateral line cells. *Methods (San Diego, Calif.)*, *62*(3), 226–231. https://doi.org/10.1016/j.ymeth.2013.06.005

Gibert, Y., & Ward, M. C. T. and A. C. (2013). Zebrafish As a Genetic Model in Pre-Clinical Drug Testing and Screening. *Current Medicinal Chemistry*, Vol. 20, pp. 2458–2466. https://doi.org/http://dx.doi.org/10.2174/0929867311320190005

Gill, C., Phelan, J. P., Hatzipetros, T., Kidd, J. D., Tassinari, V. R., Levine, B., … Vieira, F. G. (2019). SOD1-positive aggregate accumulation in the CNS predicts slower disease progression and increased longevity in a mutant SOD1 mouse model of MND. *Scientific Reports*, *9*(1), 6724. https://doi.org/10.1038/s41598-019-43164-z

Goll, M. G., Anderson, R., Stainier, D. Y. R., Spradling, A. C., & Halpern, M. E. (2009). Transcriptional silencing and reactivation in transgenic zebrafish. *Genetics*, *182*(3), 747–755. https://doi.org/10.1534/genetics.109.102079

Guigó, R., Dermitzakis, E. T., Agarwal, P., Ponting, C. P., Parra, G., Reymond, A., … Brent, M. R. (2003). Comparison of mouse and human genomes followed by experimental verification yields an estimated 1,019 additional genes. *Proceedings of the National Academy of Sciences*, *100*(3), 1140 LP – 1145. https://doi.org/10.1073/pnas.0337561100

Hammerschmidt, M., & Nusslein-Volhard, C. (1993). The expression of a zebrafish gene homologous to Drosophila snail suggests a conserved function in invertebrate and vertebrate gastrulation. *Development*, *119*(4), 1107 LP – 1118. Retrieved from

http://dev.biologists.org/content/119/4/1107.abstract

He, S., Salas-Vidal, E., Rueb, S., Krens, S. F. G., Meijer, A. H., Snaar-Jagalska, B. E., & Spaink, H. P. (2006). Genetic and Transcriptome Characterization of Model Zebrafish Cell Lines. *Zebrafish*, *3*(4), 441–453. https://doi.org/10.1089/zeb.2006.3.441

Howe, K., Clark, M. D., Torroja, C. F., Torrance, J., Berthelot, C., Muffato, M., … Stemple, D. L. (2013). The zebrafish reference genome sequence and its relationship to the human genome. *Nature*, *496*(7446), 498–503. https://doi.org/10.1038/nature12111

Huang, C., Tong, J., Bi, F., Wu, Q., Huang, B., Zhou, H., & Xia, X.-G. (2012). Entorhinal cortical neurons are the primary targets of FUS mislocalization and ubiquitin aggregation in FUS transgenic rats. *Human Molecular Genetics*, *21*(21), 4602–4614. https://doi.org/10.1093/hmg/dds299

Janus, C., & Welzl, H. (2010). *Mouse Models of Neurodegenerative Diseases: Criteria and General Methodology BT - Mouse Models for Drug Discovery: Methods and Protocols* (G. Proetzel & M. V Wiles, Eds.). https://doi.org/10.1007/978-1-60761-058-8_19

Kaur, G., & Dufour, J. M. (2012). Cell lines: Valuable tools or useless artifacts. *Spermatogenesis*, *2*(1), 1–5. https://doi.org/10.4161/spmg.19885

Klionsky, D. J., Abdelmohsen, K., Abe, A., Abedin, M. J., Abeliovich, H., Acevedo Arozena, A., … Zughaier, S. M. (2016). Guidelines for the use and interpretation of assays for monitoring autophagy (3rd edition). *Autophagy*, *12*(1), 1–222. https://doi.org/10.1080/15548627.2015.1100356

Kwiatkowski, T. J., Bosco, D. A., LeClerc, A. L., Tamrazian, E., Vanderburg, C. R., Russ, C., … Brown, R. H. (2009). Mutations in the FUS/TLS Gene on Chromosome 16 Cause Familial Amyotrophic Lateral Sclerosis. *Science*, *323*(5918), 1205 LP – 1208. https://doi.org/10.1126/science.1166066

Lanson Jr, N. A., Maltare, A., King, H., Smith, R., Kim, J. H., Taylor, J. P., … Pandey, U. B. (2011). A Drosophila model of FUS-related neurodegeneration reveals genetic interaction between FUS and TDP-43. *Human Molecular Genetics*, *20*(13), 2510–2523. https://doi.org/10.1093/hmg/ddr150

Lebedeva, S., de Jesus Domingues, A. M., Butter, F., & Ketting, R. F. (2017). Characterization of genetic loss-of-function of Fus in zebrafish. *RNA Biology*, *14*(1), 29–35. https://doi.org/10.1080/15476286.2016.1256532

Li, J., Huang, K., & Le, W. (2013). Establishing a novel C. elegans model to investigate the role of autophagy in amyotrophic lateral sclerosis. *Acta Pharmacologica Sinica*, *34*(5), 644–650. https://doi.org/10.1038/aps.2012.190

Madji Hounoum, B., Vourc'h, P., Felix, R., Corcia, P., Patin, F., Guéguinou, M., … Blasco, H. (2016). NSC-34 Motor Neuron-Like Cells Are Unsuitable as Experimental Model for Glutamate-Mediated Excitotoxicity. *Frontiers in Cellular Neuroscience*, *10*, 118. https://doi.org/10.3389/fncel.2016.00118

Marrone, L., Drexler, H. C. A., Wang, J., Tripathi, P., Distler, T., Heisterkamp, P., … Sterneckert, J. (2019). FUS pathology in MND is linked to alterations in multiple MND-

associated proteins and rescued by drugs stimulating autophagy. *Acta Neuropathologica*. https://doi.org/10.1007/s00401-019-01998-x

Mathai, B. J., Meijer, A. H., & Simonsen, A. (2017, September). Studying Autophagy in Zebrafish. *Cells*, Vol. 6. https://doi.org/10.3390/cells6030021

Mauthe, M., Orhon, I., Rocchi, C., Zhou, X., Luhr, M., Hijlkema, K.-J., … Reggiori, F. (2018). Chloroquine inhibits autophagic flux by decreasing autophagosome-lysosome fusion. *Autophagy*, *14*(8), 1435–1455. https://doi.org/10.1080/15548627.2018.1474314

McDermott, C. J., & Shaw, P. J. (2008). Diagnosis and management of motor neurone disease. *BMJ (Clinical Research Ed.)*, *336*(7645), 658–662. https://doi.org/10.1136/bmj.39493.511759.BE

McGurk, L., Berson, A., & Bonini, N. M. (2015). Drosophila as an In Vivo Model for Human Neurodegenerative Disease. *Genetics*, *201*(2), 377–402. https://doi.org/10.1534/genetics.115.179457

Murakami, T., Qamar, S., Lin, J. Q., Schierle, G. S. K., Rees, E., Miyashita, A., … St George-Hyslop, P. (2015). MND/FTD Mutation-Induced Phase Transition of FUS Liquid Droplets and Reversible Hydrogels into Irreversible Hydrogels Impairs RNP Granule Function. *Neuron*, *88*(4), 678–690. https://doi.org/10.1016/j.neuron.2015.10.030

Murakami, T., Yang, S.-P., Xie, L., Kawano, T., Fu, D., Mukai, A., … St George-Hyslop, P. (2012). MND mutations in FUS cause neuronal dysfunction and death in Caenorhabditis elegans by a dominant gain-of-function mechanism. *Human Molecular Genetics*, *21*(1), 1–9. https://doi.org/10.1093/hmg/ddr417

Nixon, R. A. (2013). The role of autophagy in neurodegenerative disease. *Nature Medicine*, *19*, 983. Retrieved from http://dx.doi.org/10.1038/nm.3232

Nolan, M., Talbot, K., & Ansorge, O. (2016). Pathogenesis of FUS-associated MND and FTD: insights from rodent models. *Acta Neuropathologica Communications*, *4*(1), 99. https://doi.org/10.1186/s40478-016-0358-8

Park, D., Jeong, H., Lee, M. N., Koh, A., Kwon, O., Yang, Y. R., … Ryu, S. H. (2016). Resveratrol induces autophagy by directly inhibiting mTOR through ATP competition. *Scientific Reports*, *6*, 21772. Retrieved from https://doi.org/10.1038/srep21772

Patel, A., Lee, H. O., Jawerth, L., Maharana, S., Jahnel, M., Hein, M. Y., … Alberti, S. (2015). A Liquid-to-Solid Phase Transition of the MND Protein FUS Accelerated by Disease Mutation. *Cell*, *162*(5), 1066–1077. https://doi.org/10.1016/j.cell.2015.07.047

Phillips, J. B., & Westerfield, M. (2014). Zebrafish models in translational research: tipping the scales toward advancements in human health. *Disease Models & Mechanisms*, *7*(7), 739–743. https://doi.org/10.1242/dmm.015545

Ramesh, N., & Pandey, U. B. (2017). Autophagy Dysregulation in MND: When Protein Aggregates Get Out of Hand. *Frontiers in Molecular Neuroscience*, *10*, 263. https://doi.org/10.3389/fnmol.2017.00263

Ryu, A. H., Eckalbar, W. L., Kreimer, A., Yosef, N., & Ahituv, N. (2017). Use antibiotics in cell culture with caution: genome-wide identification of antibiotic-induced changes in gene expression and regulation. *Scientific Reports*, *7*(1), 7533. https://doi.org/10.1038/s41598-017-07757-w

Sacitharan, P. K., Lwin, S., Gharios, G. B., & Edwards, J. R. (2018). Spermidine restores dysregulated autophagy and polyamine synthesis in aged and osteoarthritic chondrocytes via EP300. *Experimental & Molecular Medicine*, *50*(9), 123. https://doi.org/10.1038/s12276-018-0149-3

Sakowski, S. A., Lunn, J. S., Busta, A. S., Palmer, M., Dowling, J. J., & Feldman, E. L. (2012). A novel approach to study motor neurons from zebrafish embryos and larvae in culture. *Journal of Neuroscience Methods*, *205*(2), 277–282. https://doi.org/10.1016/j.jneumeth.2012.01.007

Sassen, W. A., Lehne, F., Russo, G., Wargenau, S., Dübel, S., & Köster, R. W. (2017). Embryonic zebrafish primary cell culture for transfection and live cellular and subcellular imaging. *Developmental Biology*, *430*(1), 18–31. https://doi.org/https://doi.org/10.1016/j.ydbio.2017.07.014

Scekic-Zahirovic, J., Sendscheid, O., El Oussini, H., Jambeau, M., Sun, Y., Mersmann, S., … Dupuis, L. (2016). Toxic gain of function from mutant FUS protein is crucial to trigger cell autonomous motor neuron loss. *The EMBO Journal*, *35*(10), 1077–1097. https://doi.org/10.15252/embj.201592559

Schwartz, J. C., Wang, X., Podell, E. R., & Cech, T. R. (2013). RNA seeds higher-order assembly of FUS protein. *Cell Reports*, *5*(4), 918–925. https://doi.org/10.1016/j.celrep.2013.11.017

Shang, Y., & Huang, E. J. (2016). Mechanisms of FUS mutations in familial amyotrophic lateral sclerosis. *Brain Research*, *1647*, 65–78. https://doi.org/https://doi.org/10.1016/j.brainres.2016.03.036

Sharma, A., Lyashchenko, A. K., Lu, L., Nasrabady, S. E., Elmaleh, M., Mendelsohn, M., … Shneider, N. A. (2016). MND-associated mutant FUS induces selective motor neuron degeneration through toxic gain of function. *Nature Communications*, *7*, 10465. https://doi.org/10.1038/ncomms10465

Singer, A., Eagle, A., Van Slyke, C., Pich, C., Fashena, D., Paddock, H., … Howe, D. G. (2016). The Zebrafish Model Organism Database: new support for human disease models, mutation details, gene expression phenotypes and searching. *Nucleic Acids Research*, *45*(D1), D758–D768. https://doi.org/10.1093/nar/gkw1116

Soo, K. Y., Sultana, J., King, A. E., Atkinson, R., Warraich, S. T., Sundaramoorthy, V., … Atkin, J. D. (2015). MND-associated mutant FUS inhibits macroautophagy which is restored by overexpression of Rab1. *Cell Death Discovery*, *1*, 15030. https://doi.org/10.1038/cddiscovery.2015.30

Spires-Jones, T. L., Attems, J., & Thal, D. R. (2017). Interactions of pathological proteins in neurodegenerative diseases. *Acta Neuropathologica*, *134*(2), 187–205. https://doi.org/10.1007/s00401-017-1709-7

Thomas, P., & Smart, T. G. (2005). HEK293 cell line: A vehicle for the expression of recombinant proteins. *Journal of Pharmacological and Toxicological Methods*, *51*(3), 187–200. https://doi.org/https://doi.org/10.1016/j.vascn.2004.08.014

Traynor, B. J., Codd, M. B., Corr, B., Forde, C., Frost, E., & Hardiman, O. M. (2000). Clinical Features of Amyotrophic Lateral Sclerosis According to the El Escorial and Airlie House Diagnostic Criteria: A Population-Based Study. *Archives of Neurology*, *57*(8), 1171–1176. https://doi.org/10.1001/archneur.57.8.1171

Turner, M. R., Parton, M. J., Shaw, C. E., Leigh, P. N., & Al-Chalabi, A. (2003). Prolonged survival in motor neuron disease: a descriptive study of the King's database 1990–2002. *Journal of Neurology, Neurosurgery &Amp; Psychiatry*, *74*(7), 995 LP – 997. https://doi.org/10.1136/jnnp.74.7.995

Vaccaro, A., Patten, S. A., Ciura, S., Maios, C., Therrien, M., Drapeau, P., … Parker, J. A. (2012). Methylene blue protects against TDP-43 and FUS neuronal toxicity in C. elegans and D. rerio. *PloS One*, *7*(7), e42117–e42117. https://doi.org/10.1371/journal.pone.0042117

Vaccaro, A., Tauffenberger, A., Aggad, D., Rouleau, G., Drapeau, P., & Parker, J. A. (2012). Mutant TDP-43 and FUS cause age-dependent paralysis and neurodegeneration in C. elegans. *PloS One*, *7*(2), e31321–e31321. https://doi.org/10.1371/journal.pone.0031321

van Es, M. A., Hardiman, O., Chio, A., Al-Chalabi, A., Pasterkamp, R. J., Veldink, J. H., & van den Berg, L. H. (2017). Amyotrophic lateral sclerosis. *The Lancet*, *390*(10107), 2084–2098. https://doi.org/10.1016/S0140-6736(17)31287-4

Wang, H., & Hegde, M. L. (2019). New Mechanisms of DNA Repair Defects in Fused in Sarcoma-Associated Neurodegeneration: Stage Set for DNA Repair-Based Therapeutics? *Journal of Experimental Neuroscience*, *13*, 1179069519856358–1179069519856358. https://doi.org/10.1177/1179069519856358

Wang, I.-F., Guo, B.-S., Liu, Y.-C., Wu, C.-C., Yang, C.-H., Tsai, K.-J., & Shen, C.-K. J. (2012). Autophagy activators rescue and alleviate pathogenesis of a mouse model with proteinopathies of the TAR DNA-binding protein 43. *Proceedings of the National Academy of Sciences of the United States of America*, *109*(37), 15024–15029. https://doi.org/10.1073/pnas.1206362109

Wang, I.-F., Tsai, K.-J., & Shen, C.-K. J. (2013). Autophagy activation ameliorates neuronal pathogenesis of FTLD-U mice: a new light for treatment of TARDBP/TDP-43 proteinopathies. *Autophagy*, *9*(2), 239–240. https://doi.org/10.4161/auto.22526

Whiten, D. R., San Gil, R., McAlary, L., Yerbury, J. J., Ecroyd, H., & Wilson, M. R. (2016). Rapid flow cytometric measurement of protein inclusions and nuclear trafficking. *Scientific Reports*, *6*(1), 31138. https://doi.org/10.1038/srep31138

Wolozin, B., Gabel, C., Ferree, A., Guillily, M., & Ebata, A. (2011). Watching worms whither: modeling neurodegeneration in C. elegans. *Progress in Molecular Biology and Translational Science*, *100*, 499–514. https://doi.org/10.1016/B978-0-12-384878-9.00015-7

Xi, Y., Noble, S., & Ekker, M. (2011). Modeling neurodegeneration in zebrafish. *Current*

Neurology and Neuroscience Reports, *11*(3), 274–282. https://doi.org/10.1007/s11910-011-0182-2

Appendix A of this thesis has been removed as it may contain sensitive/confidential content